Inverting the Fourier transform, we have finally

$$\nu(x=0^+)=\frac{1}{\pi}\int_{-\infty}^{\infty}\nu^+(y)dy=(\delta/\pi)^2. \tag{A10}$$

Integral equation (95) can be solved in exactly the same way, by introducing λ_1 and λ_2 for $x>0$ or $x<0$, as before. We have then, instead of (94),

$$\lambda_1(x)+\lambda_2(x)=ge^{-(1/2-\delta/\omega)x}\theta(x)-\int_{-\infty}^{\infty}\frac{\tan\delta\sinh(\delta/\pi)(x-x')}{2\pi\sinh\frac{1}{2}(x-x')}\lambda_1(x')dx', \tag{A11}$$

where θ is the step function. Its Fourier-transformed version is

$$\lambda^+(y)Y^+(y)+\lambda^-(y)Y^-(y)=\frac{gY^-(y)}{\frac{1}{2}-\delta/\pi-iy}, \tag{A12}$$

giving for $\lambda^+(y)$,

$$\lambda^+(y)=\frac{\eta Y^-(-i(\frac{1}{2}-\delta/\pi))}{(\frac{1}{2}-\delta/\pi-iy)Y^+(y)}. \tag{A13}$$

For $\lambda(0^+)$ one finds

$$\lambda(0^+)=\frac{1}{\pi}\int_{-\infty}^{\infty}\lambda^+(y)dy=gY^-\left(-i\left(\frac{1}{2}-\frac{\delta}{\pi}\right)\right). \tag{A14}$$

PHYSICAL REVIEW VOLUME 185, NUMBER 2 10 SEPTEMBER 1969

Propagation of Light Pulses in a Laser Amplifier*

A. Icsevgi† and W. E. Lamb, Jr.
Yale University, New Haven, Connecticut 06520
(Received 1 May 1969)

The problem of a light pulse propagating in a nonlinear laser medium is investigated. The electromagnetic field is treated classically and the active medium consists of thermally moving atoms which have two electronic states with independent decay constants γ_a and γ_b in addition to the decay constant γ_{ab} describing the phase memory. The self-consistency requirement that the field sustained by the polarized medium be equal to the field inducing the polarization leads to coupled equations of motion for the density matrix, and equations of propagation for the electromagnetic field. Although the theory is developed for a Doppler-broadened gaseous medium, it may also be applied to a solid medium with inhomogeneous broadening. A unified treatment is given encompassing a wide range of pulse durations from cw signals to psec pulses. Continuous pumping is allowed, as well as any amount of detuning of the carrier frequency of the pulse from the atomic resonance frequency. The three independent decay constants γ_a, γ_b, and γ_{ab} provide greater flexibility than that obtained by using $1/T_1$ and $1/T_2$. The equations are solved analytically in a few specialized cases and numerically in the general case. Flow charts for accomplishing the numerical integration are given. Among the special problems considered is the apparent paradox of pulses propagating faster than the velocity of light under circumstances described by Basov *et al.* It is shown that this contradiction with relativity arises from the use of an unphysical initial condition.

I. INTRODUCTION

We present a theoretical investigation of the behavior of light pulses traveling in an amplifying laser medium. A semiclassical description of the interaction between matter and radiation will be used, treating the medium quantum mechanically and the radiation field according to Maxwell's theory. The basic ideas are derived from Lamb's theory of optical masers.[1] However, some of his original assumptions and restrictions are relaxed in order to properly apply the theory to the problem at hand. Since there are differences between the problems of a self-sustained oscillator and of an amplifier, it is desirable to develop the theory from first principles.

The medium shall be considered to be a collection of two-level "atoms" (Fig. 1) coupled only through their interaction with the over-all radiation field. If a population inversion between the levels a and b is established, such a medium is capable of amplifying light in a frequency band around the separation of the levels.

In order to carry out necessary statistical summations, it is convenient to represent the state of a two-level atom by means of a 2×2 density matrix ρ. This is related to the wave function description in the follow-

* Research sponsored by Yale University, the Air Force Office of Scientific Research under AFOSR Grant No. 1324-67, and the NASA under Grant No. NASA-NGR 07-004-035.

† This paper is based on material submitted by A. Icsevgi in partial fulfillment of the requirements for the degree of Doctor of Philosophy at Yale University.

[1] W. E. Lamb, Jr., Phys. Rev. 134, A1429 (1964).

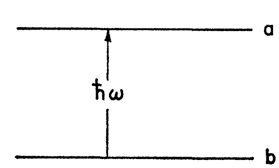

Fig. 1. Energy diagram of the two-level atom. The levels have a resonance transition frequency $\omega>0$.

ing way. Given two time-independent basis functions Ψ_a, Ψ_b, for the states a and b, the wave function for the atom can be written as

$$\Psi(t)=a(t)\Psi_a+b(t)\Psi_b\,, \tag{1}$$

and the density matrix for such a "pure case" is

$$\rho(t)\equiv\begin{pmatrix}\rho_{aa} & \rho_{ab}\\ \rho_{ba} & \rho_{bb}\end{pmatrix}=\begin{pmatrix}aa^* & ab^*\\ a^*b & bb^*\end{pmatrix}. \tag{2}$$

The off-diagonal elements of ρ will be related to the atomic dipole moment, while the diagonal elements give the probabilities for the atom to be in state a or b.

One wishes to describe the decay of the levels a, b and the damping of the atomic dipole moment. It can be shown, using the Wigner-Weisskopf theory,[2] that for radiative decay this can be achieved phenomenologically by introducing two damping constants γ_a, γ_b such that in the absence of electric field perturbations, the amplitudes a and b decay exponentially as

$$a(t)=a_0e^{-\frac{1}{2}\gamma_a t}\,, \tag{3a}$$

$$b(t)=b_0e^{-\frac{1}{2}\gamma_b t}. \tag{3b}$$

This implies that ρ_{aa}, ρ_{bb}, ρ_{ab} have decay constants γ_a, γ_b, $\gamma_{ab}=\frac{1}{2}(\gamma_a+\gamma_b)$, respectively. When the contributions to γ_a, γ_b, γ_{ab} of damping mechanisms of nonradiative type, such as phonon interruptions in solids or atomic collisions in gases, are taken into account, the simple relationship between the three constants is destroyed. One finds typically that[3]

$$\gamma_{ab}\geq\tfrac{1}{2}(\gamma_a+\gamma_b)\,. \tag{4}$$

We shall therefore regard γ_a, γ_b, and γ_{ab} as independent. The quantity γ_{ab} represents the decay constant for the dipole moment of the atom, so that $1/\gamma_{ab}$ measures the time of atomic phase memory or coherence. Associated with this damping mechanism is a spectral linewidth γ_{ab} which is sometimes called "homogeneous."

An additional broadening of a different nature is obtained when one considers an ensemble of atoms. In solids the atoms may have slightly different resonance frequencies due to inhomogeneities in the crystal environment. The averaging over resonance frequencies leads to a decay of the polarization or an "inhomogeneous broadening." In gases the averaging over various atomic velocities leads to a similar effect called "Doppler broadening." These complications will be dealt with in a more fundamental way later.

Pulses covering a wide range of duration, from quasi-monochromatic light to recently produced psec pulses,[4] are now available but previous treatments have been concerned either with very broad pulses which permit the use of rate equations,[5] or with ultrashort pulses for which the phase memory time can be considered infinitely long.[6] Basov *et al.*[7] have treated the problem of pulses very broad compared to $1/\gamma_{ab}$ and very sharp with respect to $1/\gamma_a$ and $1/\gamma_b$, but only with homogeneous broadening. Other authors[8–10] have also considered the simplified case of a homogeneously broadened medium but with arbitrary $\gamma_{ab}=1/T_2$ and $\gamma_a=\gamma_b=1/T_1$. In the domain of ultrashort pulses McCall and Hahn have treated the problem of an inhomogeneously broadened attenuator.[11] The recent work of Hopf and Scully[12] deals with an inhomogeneously broadened amplifier and includes the effects of a finite phase memory time, but their analysis applies only to solid-state lasers and they mostly take $\gamma_a=\gamma_b=1/T_1\ll\gamma_{ab}=1/T_2$. It appears that the previous attempts to deal with the problems of pulse propagation in a nonlinear medium have been unnecessarily specialized. The purpose of this paper is to give a unified treatment of the many different aspects of the problem, using one formalism. The discussion is aimed at a gaseous, medium but contains the case of a solid as a special case. It is shown that to lowest order in v/c the inhomogeneous broadening of solids and the Doppler broadening of gases are formally equivalent. This result is a consequence of dealing with running waves instead of standing waves.

The paper contains seven sections. Section II sets up the general formalism, hypotheses, and equations. The subsequent sections correspond to a classification of pulses according to their duration with respect to the atomic phase memory time $1/\gamma_{ab}$ characterizing the medium. Section III deals with monochromatic waves which can be thought of as pulses of infinite duration and which afford exact solutions. Section IV treats long pulses for which rate equations can be derived. Section V considers ultrashort pulses, and Sec. VI analyzes intermediate pulses. Until this section is reached emphasis is placed on analytical methods and solutions, but in Sec. VI we deal with the most general case for which very little can be done analytically, and numerical methods are required. A digital computer program is presented which integrates the set of coupled partial differential equations governing the dynamics of the pulse in the medium. Solutions are obtained and a discussion is given of the effects of varying such param-

---

[2] V. Weisskopf and E. Wigner, Z. Physik **63**, 54 (1930).

[3] B. L. Gyorffy, M. Borenstein, and W. E. Lamb, Jr., Phys. Rev. **169**, 340 (1968).

[4] A. J. DeMaria, D. A. Stetser, and H. A. Iteynan, Appl. Phys. Letters **8**, 174 (1966).

[5] L. M. Frantz and J. S. Nodvik, J. Appl. Phys. **34**, 2346 (1963).

[6] G. L. Lamb, Phys. Letters **25A**, 181 (1967).

[7] N. G. Basov, R. V. Ambartsumyan, V. S. Zuev, P. G. Kryukov, and V. S. Letokhov, Zh. Eksperim. i Teor. Fiz. **50**, 23 (1966) [English transl.: Soviet Phys.—JETP **23**, 16 (1966)].

[8] J. P. Wittke and P. J. Warter, J. Appl. Phys. **35**, 1668 (1964).

[9] F. T. Arecchi and R. Bonifacio, J. Quant. Electron. **QE-1**, 169 (1965).

[10] C. L. Tang and B. D. Silverman, in *Physics of Quantum Electronics*, edited by P. L. Kelley, B. Lax, and P. E. Tannenwald, (McGraw-Hill Book Co., New York, 1966).

[11] S. L. McCall and E. L. Hahn, Phys. Rev. Letters **18**, 908 (1967).

[12] F. A. Hopf and M. O. Scully, Phys. Rev. **179**, 399 (1969).

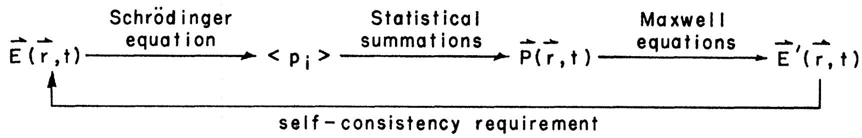

FIG. 2. Schematic basis for the derivation of the equations.

eters as decay constants, Doppler linewidth, gain, loss, pulse shape, duration and energy. The Fortran IV program used is described in Appendix G. Some derivations which would interrupt the continuity are also placed in Appendices. The last section summarizes the results of the calculations.

II. FRAMEWORK FOR ANALYSIS

A. Introduction

The scheme of calculation is well summarized by the diagram of Fig. 2. An assumed electric field $\mathbf{E}(\mathbf{r},t)$ polarizes the atoms of the medium according to the laws of quantum mechanics. The atomic dipole moments $\langle\mathbf{p}_i\rangle$ statistically add up to a macroscopic polarization $\mathbf{P}(\mathbf{r},t)$, which in turn enters Maxwell's equations as a source term and drives the electric field. In order for the scheme to be self-consistent, the electric field $\mathbf{E}'(\mathbf{r},t)$ driven by the polarization $\mathbf{P}(\mathbf{r},t)$ must be exactly equal to the assumed field $\mathbf{E}(\mathbf{r},t)$, i.e.,

$$\mathbf{E}'(\mathbf{r},t)=\mathbf{E}(\mathbf{r},t). \tag{5}$$

The calculation proceeds in three steps: (1) quantum mechanical equations for the density matrix, (2) statistical summations, (3) electromagnetic field equations.

In the remaining parts of this section we shall derive a set of coupled partial differential equations suitable for numerical integration which will be considered valid in all of the specialized cases treated in subsequent sections. In order to derive these equations we shall introduce simplifiying assumptions in two separate stages. First we assume:

(a) The two-level atoms are coupled only through their interaction with the common radiation field $\mathbf{E}(\mathbf{r},t)$.

(b) The radiation field is a scalar $E(z,t)$, representing a uniform plane wave polarized in the x direction, and propagating in the z direction (Fig. 3).

(c) The dipole approximation holds for the interaction of the atoms with the radiation field.

B. Equations of Motion for the Medium

The density matrix for a two-level atom was introduced in Sec. I. In Dirac's notation, the representation-free definition of the density matrix is

$$\rho=|\psi\rangle\langle\psi|. \tag{6}$$

The expectation value for an operator $\mathcal{O}$ is given by

$$\langle\mathcal{O}\rangle=\mathrm{Tr}(\rho\mathcal{O}). \tag{7}$$

The ket $|\Psi\rangle$ obeys Schrödinger's equation

$$i\hbar\frac{\partial}{\partial t}|\Psi\rangle=[H_0+H_{\mathrm{int}}(t)]|\Psi\rangle=H|\Psi\rangle, \tag{8}$$

where H_0 is the Hamiltonian for the unperturbed atom, and

$$H_{\mathrm{int}}=-E\mathcal{P} \tag{9}$$

is the electric field perturbation in the dipole approximation, $\mathcal{P}$ being the dipole moment operator of the atom. Differentiating (6), using (8) and its complex conjugate, we obtain

$$i\hbar\frac{\partial\rho}{\partial t}=[H,\rho]. \tag{10}$$

In the representation for which the basis functions Ψ_a, Ψ_b are eigenfunctions of H_0, we have

$$H_0=\hbar\begin{pmatrix}\omega_a & 0\\ 0 & \omega_b\end{pmatrix} \tag{11}$$

and

$$H_{\mathrm{int}}=\hbar\begin{pmatrix}0 & -(p/\hbar)E(t)\\ -(p/\hbar)E(t) & 0\end{pmatrix}, \tag{12}$$

where the matrix element

$$p=\langle a|\mathcal{P}|b\rangle=\langle b|\mathcal{P}|a\rangle \tag{13}$$

is taken to be real without loss of generality. The diagonal matrix elements of $\mathcal{P}$ vanish by parity consideration. In component form, the equation of motion (10) becomes

$$\dot\rho_{aa}=-\gamma_a\rho_{aa}-i(pE/\hbar)(\rho_{ab}-\rho_{ba}), \tag{14a}$$

$$\dot\rho_{bb}=-\gamma_b\rho_{bb}+i(pE/\hbar)(\rho_{ab}-\rho_{ba}), \tag{14b}$$

$$\dot\rho_{ab}=-(\gamma_{ab}+i\omega)\rho_{ab}-i(pE/\hbar)(\rho_{aa}-\rho_{bb}), \tag{14c}$$

$$\rho_{ba}=\rho_{ab}^*, \tag{14d}$$

where the resonance frequency ω is

$$\omega=\omega_a-\omega_b, \tag{15}$$

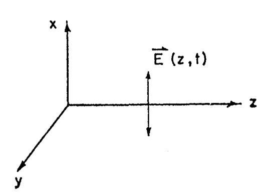

FIG. 3. Linearly polarized plane wave.

and γ_a, γ_b, γ_{ab} have been introduced phenomenologically in order to account for the correct damping of levels a and b in the absence of the electric field perturbation.

The individual atom we have been considering may be specified by the labels

$$\{\alpha,z_0,t_0,v\},$$

where α is the state a or b to which the atom was originally excited, (z_0,t_0) is the space-time point where it was excited and v is the velocity it had. We shall neglect atomic collision effects and hence the atomic velocity v will be a constant for each atom. (For a solid-state laser the label v could be replaced by a frequency label ω since the resonance frequency may vary from one atom to the other due to inhomogeneities in the crystal environment.) The density matrix for this atom has a time dependence so that it should be written as

$$\rho=\rho(\alpha,z_0,t_0,v;\,t). \tag{16}$$

From (7), the expectation value for the atomic dipole moment $\mathcal{P}$ is readily seen to be

$$\langle\mathcal{P}\rangle=p[\rho_{ab}(\alpha,z_0,t_0,v;\;t)+\rho_{ba}]. \tag{17}$$

The macroscopic polarization of the medium at (z,t), $P(z,t)$, will be produced by an ensemble of atoms which arrived at z, at time t, irrespective of their state α, place z_0, time t_0 and velocity v of excitation. The expression (16) should therefore be summed over α, z_0, t_0, v thus leading to a population matrix.

Since we have equations of motion (14) for the individual density matrices, it appears that we have to defer the summation process until $\rho(\alpha,z_0,t_0,v;\,t)$ is determined from those equations. However we will be able to sum over α, z_0, t_0 (but not v) before we integrate the equations. This is achieved in the following way. Consider

$$\rho(v,z,t)=\sum_{\alpha=a}^{b}\int_{-\infty}^{t}dt_0\int dz_0\lambda_\alpha(v,z_0,t_0)\rho(\alpha,z_0,t_0,v;\,t)\times\delta(z-z_0-v(t-t_0)), \tag{18}$$

where $\lambda_\alpha(v,z_0,t_0)$ is the number of atoms excited to state α, per unit time and unit volume. Assuming that this quantity varies slowly with z_0 and t_0, it can be taken outside the integrals and replaced by $\lambda_\alpha(v,z,t)$. The δ function in (18) insures that we are only summing over atoms which will reach the right place z at time t. Hence, $\rho(v,z,t)$ is the population matrix at time t, for a group of atoms of a given velocity v, which will be at z at time t, irrespective of their α, z_0, t_0. It is convenient to define the partial polarization produced by such a group of atoms as

$$P(v,z,t)=p[\rho_{ab}(v,z,t)+\text{c.c.}]. \tag{19}$$

The total polarization $P(z,t)$ is the sum over these partial polarizations

$$P(z,t)=\int dv\,P(v,z,t). \tag{20}$$

The integration over z_0 involved in (18) is straightforward and gives

$$\rho(v,z,t)=\sum_{\alpha=a}^{b}\lambda_\alpha\int_{-\infty}^{t}dt_0\rho(\alpha,\,z-v(t-t_0),\,t_0,\,v;\,t). \tag{21}$$

The set of equations (14) can be written more explicitly as

$$(\partial/\partial t)\rho_{aa}(\alpha,z_0,t_0,v;\,t)=-\gamma_a\rho_{aa}-i(p/\hbar)E(z_0+v(t-t_0),t)(\rho_{ab}-\rho_{ba}), \tag{22a}$$

$$(\partial/\partial t)\rho_{bb}(\alpha,z_0,t_0,v;\,t)=-\gamma_b\rho_{bb}+i(p/\hbar)E(z_0+v(t-t_0),t)(\rho_{ab}-\rho_{ba}), \tag{22b}$$

$$(\partial/\partial t)\rho_{ab}(\alpha,z_0,t_0,v;\,t)=-(\gamma_{ab}+i\omega)\rho_{ab}-i(p/\hbar)E(z_0+v(t-t_0),t)\times(\rho_{aa}-\rho_{bb}). \tag{22c}$$

Let us consider the quantity $(\partial/\partial t)\rho(v,z,t)+v(\partial/\partial z)\times\rho(v,z,t)$. In order to avoid a confusion of symbols, we would like to remind the reader that by $(\partial/\partial t)\times\rho(\alpha,z_0,t_0,v;\,t)$ we mean the derivative of ρ with respect to its fifth variable, evaluated at the given values of the arguments. Similarly, $(\partial/\partial z_0)\rho(\alpha,z_0,t_0,v;\,t)$ will mean the derivative of ρ with respect to its second variable. Introducing the symbol

$$\partial=(\partial/\partial t)+v(\partial/\partial z), \tag{23}$$

and using (21) we have

$$\begin{aligned}\partial\rho(v,z,t)=&\sum_{\alpha=a}^{b}\lambda_\alpha\rho(\alpha,z,t,v;\,t)\\&+\sum_{\alpha=a}^{b}\lambda_\alpha\int_{-\infty}^{t}dt_0\{(\partial/\partial t)\rho(\alpha,\,z-v(t-t_0),\,t_0,\,v;\,t)\\&-v(\partial/\partial z_0)\rho(\alpha,\,z-v(t-t_0),\,t_0,\,v;\,t)\\&+v(\partial/\partial z_0)\rho(\alpha,\,z-v(t-t_0),\,t_0,\,v;\,t)\};\end{aligned} \tag{24}$$

or

$$\partial\rho(v,z,t)=\sum_{\alpha=a}^{b}\lambda_\alpha\rho(\alpha,z,t,v;\,t)+\sum_{\alpha=a}^{b}\lambda_\alpha\int_{-\infty}^{t}dt_0(\partial/\partial t)\rho(\alpha,\,z-v(t-t_0),\,t_0,\,v;\,t). \tag{25}$$

From (22) it is found for example that

$$\begin{aligned}(\partial/\partial t)\rho_{aa}(\alpha,\,z-v(t-t_0),\,t_0,\,v;\,t)&\\=-\gamma_a\rho_{aa}(\alpha,\,z-v(t-t_0),\,t_0,\,v;\,t)&\\-i(p/\hbar)E(z-v(t-t_0)+v(t-t_0),\,t)&\\\times[\rho_{ab}(\alpha,\,z-v(t-t_0),\,t_0,\,v;\,t)-\text{c.c.}].&\end{aligned} \tag{26}$$

On the other hand, we have

$$\rho(\alpha,z,t,v;t)=\begin{pmatrix}\delta_{a\alpha} & 0\\ 0 & \delta_{b\alpha}\end{pmatrix},\qquad(27)$$

and

$$\sum_{\alpha=a}^{b}\lambda_\alpha\rho(\alpha,z,t,v;t)=\begin{pmatrix}\lambda_a & 0\\ 0 & \lambda_b\end{pmatrix},\qquad(28)$$

so that the *aa* component of Eq. (25) becomes

$$\partial\rho_{aa}(v,z,t)=\lambda_a-\gamma_a\rho_{aa}-i(p/\hbar)E(z,t)\times[\rho_{ab}(v,z,t)-\text{c.c.}],\qquad(29)$$

and similarly for the other components. We can write these equations in a more compact form as

$$\partial\rho_{aa}(v,z,t)=\lambda_a-\gamma_a\rho_{aa}-i(p/\hbar)E(z,t)(\rho_{ab}-\rho_{ba}),\qquad(30a)$$

$$\partial\rho_{bb}(v,z,t)=\lambda_b-\gamma_b\rho_{bb}+i(p/\hbar)E(z,t)(\rho_{ab}-\rho_{ba}),\qquad(30b)$$

$$\partial\rho_{ab}(v,z,t)=-(\gamma_{ab}+i\omega)\rho_{ab}-i(p/\hbar)E(z,t)\times(\rho_{aa}-\rho_{bb}),\qquad(30c)$$

$$\rho_{ba}=\rho_{ab}^*.\qquad(30d)$$

It is desirable to rewrite these equations in terms of the partial polarization

$$P(v,z,t)=p[\rho_{ab}(v,z,t)+\text{c.c.}].\qquad(31)$$

This can be done with some algebraic manipulation left to Appendix A. The result is

$$[(\partial+\gamma_{ab})^2+\omega^2]P=-2\omega(p^2/\hbar)E(\rho_{aa}-\rho_{bb}),\qquad(32a)$$

$$(\partial+\gamma_a)\rho_{aa}=\lambda_a+(\hbar\omega)^{-1}E(\partial+\gamma_{ab})P,\qquad(32b)$$

$$(\partial+\gamma_b)\rho_{bb}=\lambda_b-(\hbar\omega)^{-1}E(\partial+\gamma_{ab})P.\qquad(32c)$$

C. Electromagnetic Field Equations

The Maxwell's equations appropriate to our case are (in mks units)

$$\nabla\cdot\mathbf{D}=0,\quad \nabla\times\mathbf{E}=-\partial\mathbf{B}/\partial t,\qquad(33a)$$

$$\nabla\cdot\mathbf{B}=0,\quad \nabla\times\mathbf{H}=\mathbf{J}+\partial\mathbf{D}/\partial t,\qquad(33b)$$

where

$$\mathbf{D}=\epsilon_0\mathbf{E}+\mathbf{P},\quad \mathbf{B}=\mu_0\mathbf{H},\quad \mathbf{J}=\sigma\mathbf{E}.\qquad(33c)$$

Here **P** is the polarization and **J** is the current density. Although the medium is assumed free of real charges and currents, a fictitious Ohmic current **J** is introduced in order to account phenomenologically for the linear losses incurred in any absorbing background medium. Taking the curl of the second Eq. (33a) and using (33b) along with $\mathbf{B}=\mu_0\mathbf{H}$, one gets

$$\nabla\times\nabla\times\mathbf{E}+\mu_0\sigma\partial\mathbf{E}/\partial t+c^{-2}\partial^2\mathbf{E}/\partial t^2=-\mu_0\partial^2\mathbf{P}/\partial t^2.\qquad(34)$$

In our case

$$\mathbf{E}(\mathbf{r},t)=E(z,t)\hat{x},\qquad(35)$$

and the above equation reduces to

$$-\partial^2E/\partial z^2+\mu_0\sigma\partial E/\partial t+c^{-2}\partial^2E/\partial t^2=-\mu_0\partial^2P/\partial t^2.\qquad(36)$$

Coupling this equation with the equations of motion (32) for the medium we get

$$-\partial^2E/\partial z^2+\mu_0\sigma\partial E/\partial t+c^{-2}\partial^2E/\partial t^2=-\mu_0\partial^2P(z,t)/\partial t^2,\qquad(37a)$$

$$[(\partial+\gamma_{ab})^2+\omega^2]P(v,z,t)=-2\omega(p^2/\hbar)E(\rho_{aa}-\rho_{bb}),\qquad(37b)$$

$$(\partial+\gamma_a)\rho_{aa}(v,z,t)=\lambda_a+(\hbar\omega)^{-1}E(\partial+\gamma_{ab})P(v,z,t),\qquad(37c)$$

$$(\partial+\gamma_b)\rho_{bb}(v,z,t)=\lambda_b-(\hbar\omega)^{-1}E(\partial+\gamma_{ab})P(v,z,t),\qquad(37d)$$

where $P(z,t)$ and $P(v,z,t)$ are related by Eq. (20). Note that Eqs. (37) were derived under assumptions (a), (b), and (c) of Sec. II A. In the special case $\gamma_a=\gamma_b=\gamma$, the last two equations combine into a single equation for the population inversion density $N=\rho_{aa}-\rho_{bb}$, namely

$$(\partial+\gamma)N=\lambda_a-\lambda_b+2(\hbar\omega)^{-1}E(\partial+\gamma_{ab})P.\qquad(38)$$

D. Reduction of the Basic Equations

Equations (37) will now be reduced on the basis of the three additional assumptions (d), (e), and (f)

(d) The optical frequency ω is much larger than the natural linewidth γ_{ab}, i.e.,

$$\omega\gg\gamma_{ab}.\qquad(39)$$

(e) The rotating wave approximation holds, i.e. harmonics of the optical frequency will be neglected.

(f) The field can adequately be represented as a running wave with slowly varying amplitude and phase

$$E(z,t)=\mathcal{E}(z,t)\cos[\nu t-Kz+\varphi(z,t)].\qquad(40)$$

In order that the reflected wave may be neglected, we shall have to assume that the properties of the medium may vary only slightly over a wavelength. The frequency ν has a nominal value close to the atomic frequency ω. (Note that ν is a distinct circular frequency and is not equal to $\omega/2\pi$.) For the problem of a laser oscillator inside a cavity, ν represented the frequency of oscillations and was determined by the equations. In our problem ν is a convenient frequency chosen to represent the incoming pulse. A pulse does not have a well-defined frequency and the choice of ν is pretty much arbitrary. Different choices of ν lead to different phase functions $\varphi(z,t)$. We shall therefore set $\nu=\omega$, without loss of generality, when we consider sufficiently short pulses. However, in the case of a nearly monochromatic wave it is convenient to keep ν arbitrary. The wave number K will always be

$$K=\nu/c.\qquad(41)$$

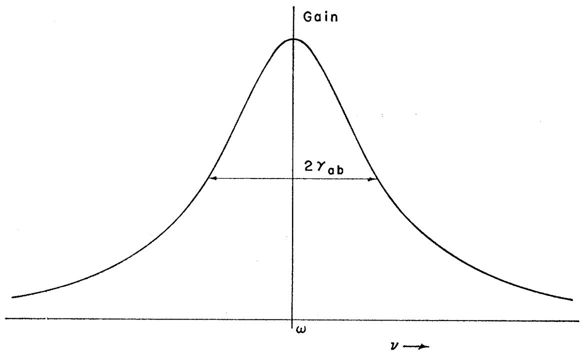

FIG. 4. Lorentzian gain profile with full width at half-maximum $=2\gamma_{ab}$.

The amplitude $\mathcal{E}$ and phase φ shall vary slowly in an optical cycle and wavelength, i.e.,

$$\partial\mathcal{E}/\partial t \ll \nu\mathcal{E}\,, \quad \partial\mathcal{E}/\partial z \ll K\mathcal{E}\,, \tag{42a}$$

$$\partial\varphi/\partial t \ll \nu\varphi\,, \quad \partial\varphi/\partial z \ll K\varphi\,. \tag{42b}$$

If the field is written as in (40), the response of the medium, neglecting higher harmonics, is of the form

$$P(v,z,t)=C(v,z,t)\cos(\nu t-kz+\varphi) +S(v,z,t)\sin(\nu t-Kz+\varphi)\,, \tag{43}$$

where C and S can be called, respectively, the in-phase and the out-of-phase components of the polarization. When these expressions are substituted into Eqs. (37) and the above approximations are made (see Appendix B) one obtains

$$\partial\mathcal{E}/\partial z+c^{-1}\partial\mathcal{E}/\partial t=-\kappa\mathcal{E}-\tfrac{1}{2}K\langle S/\epsilon_0\rangle_v\,, \tag{44a}$$

$$(\partial\varphi/\partial z+c^{-1}\partial\varphi/\partial t)\mathcal{E}=-\tfrac{1}{2}K\langle C/\epsilon_0\rangle_v\,, \tag{44b}$$

$$\partial S=-\gamma_{ab}S-(\omega-\nu+Kv-\partial\varphi)C -(p^2/\hbar)\mathcal{E}(\rho_{aa}-\rho_{bb})\,, \tag{44c}$$

$$\partial C=-\gamma_{ab}C+(\omega-\nu+Kv-\partial\varphi)S\,, \tag{44d}$$

$$\partial\rho_{aa}=\Lambda_a-\gamma_a\rho_{aa}+\tfrac{1}{2}\mathcal{E}S/\hbar\,, \tag{44e}$$

$$\partial\rho_{bb}=\Lambda_b-\gamma_b\rho_{bb}-\tfrac{1}{2}\mathcal{E}S/\hbar\,, \tag{44f}$$

where

$$\kappa=\tfrac{1}{2}\sigma/\epsilon_0 c \tag{45}$$

is the linear loss coefficient, the symbol $\langle\ \rangle_v$ stands for

$$\langle\cdots\rangle_v=\int(\cdots)W(v)dv\,, \tag{46}$$

the velocity independent source terms Λ_a, Λ_b are such that

$$\lambda_\alpha(v,z,t)=\Lambda_\alpha(z,t)W(v)\,, \tag{47}$$

and $W(v)$ is the velocity distribution function. Atomic motion affects Eqs. (44) in two ways. The Kv terms correspond to the Doppler shift in the frequency seen by the atom and play formally the same role as a $\Delta\omega$ for a solid-state medium. But there are also terms involving $v(\partial/\partial z)$. These formally distinguish the problem of a gaseous amplifier from the problem of a solid-state amplifier for which they would not appear. The physical meaning of the $v(\partial/\partial z)$ terms is that, given an atom of velocity v and its state at some space-time point (z_0,t_0), we can only predict its polarization state at subsequent space time points (z,t) for which $z-z_0=v(t-t_0)$. This is a reasonable result because in our model (constant v) the atom will never leave this path and we would expect to predict its state only at those points which it can reach. Although the $v(\partial/\partial z)$ terms are logically necessary, it can be shown that they are small correction terms that can be neglected. This is seen as follows. If L and $\Delta\tau$ are the length and duration of the pulse related by $L\sim c\Delta\tau$, one has

$$\partial/\partial t\sim 1/\Delta\tau\,, \quad \partial/\partial z\sim 1/L\,, \tag{48}$$

hence,

$$\partial=(\partial/\partial t)+v(\partial/\partial z)\sim\Delta\tau^{-1}+vL^{-1} \sim\Delta\tau^{-1}[1+(v/c)]\,. \tag{49}$$

Since $v/c\sim 10^{-5}$, the second terms can be neglected and we may drop the $v(\partial/\partial z)$ terms in Eqs. (44). We also use the retarded time, by transforming to new variables

$$\tau=t-z/c\,, \tag{50a}$$

$$z'=z\,, \tag{50b}$$

so that

$$\partial/\partial z+c^{-1}\partial/\partial t=\partial/\partial z'\,, \quad \partial/\partial t=\partial/\partial\tau\,, \tag{51}$$

and Eqs. (44) become

$$\partial\mathcal{E}/\partial z=-\kappa\mathcal{E}-\tfrac{1}{2}K\langle S/\epsilon_0\rangle_v\,, \tag{52a}$$

$$\mathcal{E}\partial\varphi/\partial z=-\tfrac{1}{2}K\langle C/\epsilon_0\rangle_v\,, \tag{52b}$$

$$\partial S/\partial\tau=-\gamma_{ab}S-(\omega-\nu+Kv-\dot{\varphi})C -(p^2/\hbar)\mathcal{E}(\rho_{aa}-\rho_{bb})\,, \tag{52c}$$

$$\partial C/\partial\tau=-\gamma_{ab}C+(\omega-\nu+Kv-\dot{\varphi})S\,, \tag{52d}$$

$$\partial\rho_{aa}/\partial\tau=\Lambda_a-\gamma_a\rho_{aa}+\tfrac{1}{2}\mathcal{E}S/\hbar\,, \tag{52e}$$

$$\partial\rho_{bb}/\partial\tau=\Lambda_b-\gamma_b\rho_{bb}-\tfrac{1}{2}\mathcal{E}S/\hbar\,, \tag{52f}$$

where the prime of z' has been dropped. In subsequent sections, Eqs. (52) will be used as a starting point to discuss a variety of special cases.

III. MONOCHROMATIC WAVE

A. Fixed Atoms—Homogeneous Broadening

1. Description of the Field and Polarization

The requirement for monochromaticity is met by taking a purely sinusoidal time dependence such as

$$E(z,t)=\mathcal{E}(z)\cos[\nu t-Kz+\varphi(z)]\,. \tag{53}$$

Neglecting higher-order harmonics, the response of the medium is then also monochromatic:

$$P(z,t)=C(z)\cos(\nu t-Kz+\varphi)+S(z)\sin(\nu t-Kz+\varphi). \quad (54)$$

The relevant quantities $\mathcal{E}$, φ, S, C have no time dependence in this case.

2. *Simplification of the Basic Equations*

The left-hand sides of the last four equations (52) vanish, as do the $\dot{\varphi}$ terms. One then obtains, for the single-velocity $v=0$ case

$$d\mathcal{E}/dz=-\kappa\mathcal{E}-\tfrac{1}{2}KS/\epsilon_0, \quad (55a)$$

$$\mathcal{E}d\varphi/dz=-\tfrac{1}{2}KC/\epsilon_0, \quad (55b)$$

$$\gamma_{ab}C=(\omega-\nu)S, \quad (55c)$$

$$(\omega-\nu)C+\gamma_{ab}S=-(p^2/\hbar)\mathcal{E}(\rho_{aa}-\rho_{bb}), \quad (55d)$$

$$\rho_{aa}=(\Lambda_a/\gamma_a)+\tfrac{1}{2}\mathcal{E}S/(\hbar\gamma_a), \quad (55e)$$

$$\rho_{bb}=(\Lambda_b/\gamma_b)-\tfrac{1}{2}\mathcal{E}S/(\hbar\gamma_b). \quad (55f)$$

The system of equations (55) can easily be combined to give a single equation for the field envelope $\mathcal{E}$. This is achieved in the following way. From (55c) and (55d) one finds

$$S=-(p^2/\hbar\gamma_{ab})\mathfrak{L}(\omega-\nu)\mathcal{E}(\rho_{aa}-\rho_{bb}), \quad (56)$$

where $\mathfrak{L}(\omega-\nu)$ is a dimensionless Lorentzian factor

$$\mathfrak{L}(\omega-\nu)=\gamma_{ab}^2[(\omega-\nu)^2+\gamma_{ab}^2]^{-1}. \quad (57)$$

Then (55e) and (55f) are used to obtain

$$\rho_{aa}-\rho_{bb}=N_0+\mathcal{E}S/(\hbar\gamma), \quad (58)$$

where

$$N_0=(\Lambda_a/\gamma_a)-(\Lambda_b/\gamma_b) \quad (59)$$

is the steady population inversion that would be sustained by the pumping competing with the damping in the absence of electromagnetic fields, and

$$\gamma^{-1}=\tfrac{1}{2}(\gamma_a^{-1}+\gamma_b^{-1}). \quad (60)$$

Substituting (56) in (58) and solving for $\rho_{aa}-\rho_{bb}$, we have

$$\rho_{aa}-\rho_{bb}=N_0[1+(p^2\mathcal{E}^2/\hbar^2\gamma\gamma_{ab})\mathfrak{L}(\omega-\nu)]^{-1}. \quad (61)$$

It is seen from this expression that the population inversion is unchanged to first order by a weak field and that it is saturated ($\rho_{aa}-\rho_{bb}\simeq 0$) by a strong field. The quantity

$$I=p^2\mathcal{E}^2/(\hbar^2\gamma_{ab}\gamma) \quad (62)$$

will be called the "dimensionless intensity." As seen from (61), $I\mathfrak{L}(\omega-\nu)=1$ produces 50% saturation. In terms of I, Eq. (55a) now gives

$$dI/dz=-2\kappa I+2\alpha I[1+I\mathfrak{L}(\omega-\nu)]^{-1}, \quad (63)$$

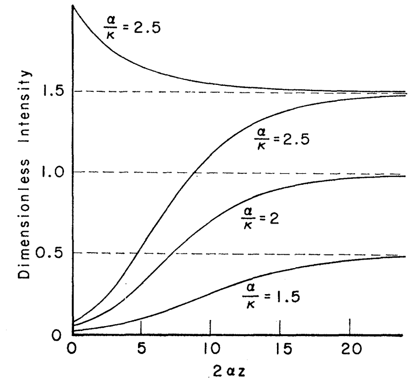

FIG. 5. Amplification of a cw signal for various values of the parameter α/κ. The uppermost curve shows the attenuation of a signal initially stronger than the limiting value. The origin along the z axis must be chosen to correspond to the initial intensity of the signal.

where

$$\alpha=GK\mathfrak{L}(\omega-\nu)=\alpha_0\mathfrak{L}(\omega-\nu) \quad (64)$$

is the small signal gain constant, and

$$G=\tfrac{1}{2}(p^2N_0/\epsilon_0\hbar\gamma_{ab}) \quad (65)$$

is a dimensionless gain parameter.

The condition for a growing solution is obviously $\alpha>\kappa$ and we shall refer to the situation $\alpha=\kappa$ as a threshold. The gain constant α has a Lorentzlan profile with FWHH$=2\gamma_{ab}$ (Fig. 4). We can deduce from (63) the "limiting intensity" I_l by setting

$$dI/dz=0=-2\kappa I_l+2\alpha I_l[1+I_l\mathfrak{L}(\omega-\nu)]^{-1}, \quad (66)$$

hence

$$I_l=[(\alpha-\kappa)/\kappa][\mathfrak{L}(\omega-\nu)]^{-1}. \quad (67)$$

The quantity $(\alpha-\kappa)/\kappa$ is just the dimensionless measure of the amount by which threshold is exceeded. From the Lorentzian factor in (67) we see that the limiting intensity is higher for an off-resonance signal, but the distance required for build-up is increased, due to the Lorentzian profile of the gain.

It is instructive to examine the condition for Eq. (63) to be approximated by the series expansion

$$dI/dz=-2\kappa I+2\alpha I[1-I\mathfrak{L}(\omega-\nu)]=2(\alpha-\kappa)I-2\alpha\mathfrak{L}(\omega-\nu)I^2. \quad (68)$$

A perturbation approach would lead to the above if carried out to third order. Equation (68) yields a limiting intensity

$$I_l=[(\alpha-\kappa)/\alpha][\mathfrak{L}(\omega-\nu)]^{-1} \quad (69)$$

smaller than the exact value (67) by a factor κ/α which is approximately unity near threshold. Hence, for operation around threshold (63) can be approximated by (68).

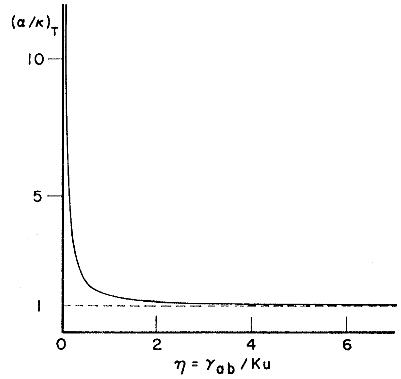

FIG. 6. Threshold value of the parameter α/κ as a function of the dimensionless quantity η.

Equation (63) can be integrated exactly and an implicit solution is

$$I|1-I/I_l|^{\alpha/\kappa}=I_0|1-I_0/I_l|^{\alpha/\kappa}e^{2(\alpha-\kappa)(z-z_0)}, \quad (70)$$

where I_0 is the value of the intensity at position $z=z_0$. A computer illustration of (70) is given in Fig. 5. As can be seen from this figure a small signal is first amplified exponentially with a net gain constant $\alpha-\kappa$, but as the signal grows, saturation effects come into play and a steady state is reached. If an intensity larger than I_l is sent into the medium, it is attenuated down to the same value I_l as is shown by one curve in Fig. 5.

The role of the linear loss κ in the dynamics of this problem is very important since $\kappa=0$ leads to solutions of a different functional form. This can be seen by taking the limit of Eq. (70) as $\kappa\rightarrow 0$, or directly by integrating (63) with $\kappa=0$. One then finds

$$Ie^{\mathcal{L}(\omega-\nu)I}=I_0e^{\mathcal{L}(\omega-\nu)I_0}e^{2\alpha(z-z_0)}. \quad (71)$$

Asymptotically, I grows like $2\alpha z$ as $z\rightarrow\infty$. This continued rise in intensity is a consequence of neglecting the linear loss mechanism.[13]

B. Moving Atoms—Doppler Broadening (Inhomogeneous Broadening)

For a given value of the velocity v, it is seen from the basic Eqs. (52) that Eqs. (55) must be generalized by formally substituting $\omega-\nu+Kv$ for $\omega-\nu$, the Doppler shift giving an effective resonance frequency equal to $\omega+Kv$. Following the steps given in the preceding paragraph and finally taking an average over the v dependence one finds that Eq. (63) generalizes to

$$dI/dz=-2\kappa I+2\alpha_0 I\langle\mathcal{L}(\omega-\nu+Kv)\times[1+I\mathcal{L}(\omega-\nu+Kv)]^{-1}\rangle_v, \quad (72)$$

where α_0 was defined by Eq. (64). We assume a Maxwellian velocity distribution

$$\langle\cdots\rangle_v=\pi^{-1/2}\int_{-\infty}^{+\infty}e^{-v^2/u^2}(\cdots)d(v/u), \quad (73)$$

and find

$$\langle\mathcal{L}(\omega-\nu+Kv)[1+I\mathcal{L}(\omega-\nu+Kv)]^{-1}\rangle_v =\pi^{-1/2}\gamma_{ab}^2\int_{-\infty}^{+\infty}e^{-v^2/u^2}[(\omega-\nu+Kv)^2+\gamma_{ab}^2(1+I)]^{-1}d(v/u). \quad (74)$$

By introducing parameters

$$\xi=(\omega-\nu)/Ku, \quad (75)$$

$$\eta=\gamma_{ab}/Ku, \quad (76)$$

and

$$x=(\gamma_{ab}/Ku)(1+I)^{1/2}, \quad (77)$$

(74) can be written as

$$\langle\ \rangle_v=\pi^{-1/2}\eta^2\int_{-\infty}^{+\infty}[(t+\xi)^2+x^2]^{-1}e^{-t^2}dt. \quad (78)$$

As shown in Appendix C, this integral can be related to the imaginary part Z_i of the plasma dispersion function

$$Z(\zeta)=i\int_0^{\infty}\exp\{-\tfrac{1}{4}\mu^2-\zeta\mu\}d\mu. \quad (79)$$

As a result (72) becomes

$$dI/dz=-2\kappa I+2\alpha_0\eta^2x^{-1}Z_i(x+i\xi)I. \quad (80)$$

It is also shown in Appendix C that in the special case of an on-resonance signal ($\omega=\nu$), the result can be expressed in terms of the error function defined as

$$\mathrm{erfc}(x)=2\pi^{-1/2}\int_x^{+\infty}e^{-t^2}dt. \quad (81)$$

Equation (80) may be replaced in this case by

$$dI/dz=-2\kappa I+2\pi^{1/2}\alpha_0\eta^2x^{-1}e^{x^2}\mathrm{erfc}(x)\,I. \quad (82)$$

Equations (80) and (82) cannot be integrated analytically. In the following discussion we shall restrict ourselves to the simpler case of Eq. (82) ($\omega=\nu$).

The solution of (82) presents the same qualitative features as (63), namely exponential growth from small values with ultimate saturation. To obtain the threshold condition as a function of η we take the limit of (82) for small I and find

$$(\alpha_0/\kappa)_T=\pi^{-1/2}e^{-\eta^2}[\eta\ \mathrm{erfc}(\eta)]^{-1}. \quad (83)$$

This result is illustrated in Fig. 6. The limiting intensity

[13] W. E. Lamb, Jr., in *Lectures in Theoretical Physics*, edited by W. E. Brittin and B. W. Downs (Interscience Publishers, Inc., New York, 1960), Vol. 2, p. 472.

is obtained from

$$0=-\kappa+\pi^{1/2}\alpha_0\eta^2 x_l^{-1}e^{x_l^2}\mathrm{erfc}(x_l). \qquad (84)$$

Given a value of η, this is numerically solved for x_l which in turn gives the limiting intensity I_l through

$$x_l^2=\eta^2(1+I_l). \qquad (85)$$

For a special choice of α_0/κ, the result is shown in Fig. 7. Using appropriate expansions of the error function it can be shown that the limiting forms of these results are

$$(\alpha_0/\kappa)_T=1+\eta^{-2}, \qquad (86)$$

and

$$I_l=[(\alpha-\kappa)/\kappa]-\eta^{-2}, \qquad (87)$$

for $\eta \ll 1$ (narrow Doppler line) and

$$(\alpha_0/\kappa)=\pi^{-1/2}\eta^{-1}, \qquad (88)$$

and

$$I_l=(\pi\eta^2\alpha_0^2/\kappa^2)-1 \qquad (89)$$

for $\eta \ll 1$ (broad Doppler line).

IV. LONG PULSES

By long pulses we mean that the spectral width of the pulse is small compared to γ_{ab}, which implies that the pulse duration $\Delta\tau_0$ is much longer than the atomic phase memory time $1/\gamma_{ab}$

$$\Delta\tau_0 \gg 1/\gamma_{ab}. \qquad (90)$$

As stated in Sec. I, $\gamma_{ab}>\frac{1}{2}(\gamma_a+\gamma_b)$, so that $1/\gamma_a$ and $1/\gamma_b$ are longer than $1/\gamma_{ab}$. This is seen in Fig. 8 which also shows the two possible ranges of pulse widths 1 and 2 that will be considered in this section.

In Case 1 we shall consider the limit

$$\Delta\tau_0 \gg 1/\gamma_a, \quad \Delta\tau_0 \gg 1/\gamma_b. \qquad (91)$$

For many gas lasers (but not CO_2), (91) is not a very restrictive condition because $1/\gamma_a$ and $1/\gamma_b$ are not much larger than $1/\gamma_{ab}$ and we have already assumed $\Delta\tau_0 \gg 1/\gamma_{ab}$. On the other hand, in the CO_2 laser and in most of the solid-state lasers, $1/\gamma_{ab}$ is commonly smaller than $1/\gamma_a$ and $1/\gamma_b$ by several orders of magnitude, and a more complete description of the behavior of "long pulses" should include both Cases 1 and 2. When we treat Case 2 we shall consider the limit

$$\Delta\tau_0 \ll 1/\gamma_a, \quad \Delta\tau_0 \ll 1/\gamma_b. \qquad (92)$$

In view of the foregoing considerations, Case 1 refers to pulse durations long compared to atomic decay times, and Case 2 to pulse durations short compared to these times.

A. Fixed Atoms (Homogeneous Broadening)

We take the field in the form

$$E(z,t)=\mathcal{E}(z,t)\cos[\nu t-Kz+\varphi(z,t)]. \qquad (93)$$

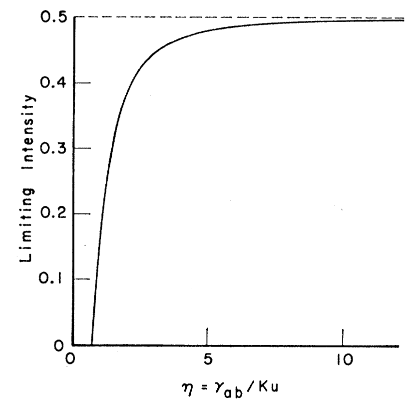

FIG. 7. The limiting intensity I_l as a function of η, for fixed $\alpha/\kappa=1.5$. The asymptotic value in the limit $\eta\to\infty$ (vanishing Doppler width) is $(\alpha-\kappa)/\kappa=0.5$. For η less than η_T the medium is below threshold for the chosen magnitude of α/κ. The value of η_T as a function of α/κ can be obtained from Fig 6.

It is again preferable to allow $\nu\neq\omega$ since a long pulse has a pretty well defined frequency. The polarization is then

$$P(z,t)=C(z,t)\cos(\nu t-Kz+\varphi)+S(z,t)\times\sin(\nu t-Kz+\varphi). \qquad (94)$$

When $v=0$, Eqs. (52) become

$$\partial\mathcal{E}/dz=-\kappa\mathcal{E}-\tfrac{1}{2}KS/\epsilon_0, \qquad (95a)$$

$$\mathcal{E}\,\partial\varphi/\partial z=-\tfrac{1}{2}KC/\epsilon_0, \qquad (95b)$$

$$\partial S/\partial\tau=-\gamma_{ab}S-(\omega-\nu-\dot{\varphi})C-(p^2/\hbar)\mathcal{E}(\rho_{aa}-\rho_{bb}), \qquad (95c)$$

$$\partial C/\partial\tau=-\gamma_{ab}C+(\omega-\nu-\dot{\varphi})S, \qquad (95d)$$

$$\partial\rho_{aa}/\partial\tau=\Lambda_a-\gamma_a\rho_{aa}+\tfrac{1}{2}\mathcal{E}S/\hbar, \qquad (95e)$$

$$\partial\rho_{bb}/\partial\tau=\Lambda_b-\gamma_b\rho_{bb}-\tfrac{1}{2}\mathcal{E}S/\hbar. \qquad (95f)$$

We now make use of the fact that $\mathcal{E}$, C, S, φ vary slowly in a time $1/\gamma_{ab}$. In this approximation the left-hand sides of (95c) and (95d), as well as the $\dot{\varphi}$ terms can be neglected. Solving these two equations for S we have

$$S=-(p^2/\hbar\gamma_{ab})\mathcal{L}(\omega-\nu)\mathcal{E}(\rho_{aa}-\rho_{bb}). \qquad (96)$$

Substituting this expression into (95a), (95e), and (95f) we obtain

$$\partial\mathcal{E}/\partial z=-\kappa\mathcal{E}+\alpha N_0^{-1}(\rho_{aa}-\rho_{bb})\mathcal{E}, \qquad (97a)$$

$$\partial\rho_{aa}/\partial\tau=\Lambda_a-\gamma_a\rho_{aa}-\tfrac{1}{2}\gamma_{ab}(p\mathcal{E}/\hbar\gamma_{ab})^2\times\mathcal{L}(\omega-\nu)(\rho_{aa}-\rho_{bb}), \qquad (97b)$$

$$\partial\rho_{bb}/\partial\tau=\Lambda_b-\gamma_b\rho_{bb}+\tfrac{1}{2}\gamma_{ab}(p\mathcal{E}/\hbar\gamma_{ab})\times\mathcal{L}(\omega-\nu)(\rho_{aa}-\rho_{bb}), \qquad (97c)$$

where α was defined by (64). The last two equations involve $\mathcal{E}^2$ which suggests that we transform (97a) into an equation for the photon flux defined as

$$\mathcal{I}=\tfrac{1}{2}\epsilon_0\mathcal{E}^2c/(\hbar\nu). \qquad (98)$$

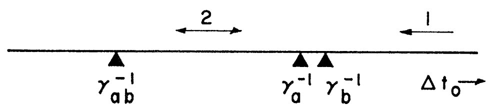

FIG. 8. Visualization of the various times involved in Sec. IV.

Multiplying (97a) by $\epsilon_0\mathcal{E}^2c/(\hbar\nu)$ we get

$$\partial\mathcal{I}/\partial z = -2\kappa\mathcal{I}+\sigma(\rho_{aa}-\rho_{bb})\mathcal{I}\,, \tag{99a}$$

$$\partial\rho_{aa}/\partial\tau+\gamma_a[\rho_{aa}-(\Lambda_a/\gamma_a)] = -\sigma(\rho_{aa}-\rho_{bb})\mathcal{I}\,, \tag{99b}$$

$$\partial\rho_{bb}/\partial\tau+\gamma_b[\rho_{bb}-(\Lambda_b/\gamma_b)] = \sigma(\rho_{aa}-\rho_{bb})\mathcal{I}\,, \tag{99c}$$

where

$$\sigma=\sigma_0\mathcal{L}(\omega-\nu)=2\alpha N_0^{-1} \tag{100}$$

is the effective cross section for stimulated emission or absorption and

$$\sigma_0=2\alpha_0N_0^{-1} \tag{101}$$

is its resonance value.

Case 1. Pulse duration long compared to atomic decay times. We now assume that the pulse width $\Delta\tau_0$ is long compared to the decay times of the states a and b, i.e., $\Delta\tau_0\gg1/\gamma_a$ and $1/\gamma_b$. This means that in (99b) and (99c) we may neglect $\partial\rho_{aa}/\partial\tau$ and $\partial\rho_{bb}/\partial\tau$ compared to $\gamma_a\rho_{aa}$ and $\gamma_b\rho_{bb}$. The equations may then be solved for

$$N=\rho_{aa}-\rho_{bb}. \tag{102}$$

After some algebra we find

$$N=N_0[1+(2\sigma/\gamma)\mathcal{I}]^{-1}, \tag{103}$$

where N_0 and γ were defined by (59) and (60). We see from (103) that

$$\mathcal{I}_s=\gamma/(2\sigma) \tag{104}$$

is the photon flux that produces 50% saturation. Substituting (103) into (99a) we obtain

$$\partial\mathcal{I}(z,t)/\partial z=-2\kappa\mathcal{I}+\sigma N_0\mathcal{I}[1+(2\sigma/\gamma)\mathcal{I}]^{-1}. \tag{105}$$

This equation is formally analogous to Eq. (63), but in the previous section the field intensity was a function of z only, thus leading to the ordinary differential Eq. (63), while in this section we have to deal with the partial differential Eq. (105) because of the additional time dependence of $\mathcal{I}$.

The condition for amplification of a small signal, i.e., threshold, is

$$\sigma N_0>2\kappa. \tag{106}$$

The limiting photon flux is readily seen to be

$$\mathcal{I}_l=[(\sigma N_0-2\kappa)/(2\kappa)][\gamma/(2\sigma)]. \tag{107}$$

The general solution of (105) is

$$\mathcal{I}(z,\tau)\,|1-[\mathcal{I}(z,\tau)/\mathcal{I}_l]|^{-\sigma N_0/(2\kappa)} = \mathcal{I}(0,\tau)\,|1-[\mathcal{I}(0,\tau)/\mathcal{I}_l]|^{-\sigma N_0/(2\kappa)} \times\exp[(\sigma N_0-2\kappa)z], \tag{108}$$

where $\mathcal{I}(0,\tau)$ is the input pulse at $z=0$. As z increases, this solution approaches the limiting intensity $\mathcal{I}_l$ defined by (107). It can be seen from (108) that the peak of the pulse travels with the velocity of light. Indeed, for any fixed z the peak of the pulse occurs for $\tau=\tau_p$ such that $\mathcal{I}(z,\tau_p)$ is a maximum and it is easily seen that this occurs when $\mathcal{I}(0,\tau)$ has also a maximum. Consequently, $\mathcal{I}(z,\tau)$ and $\mathcal{I}(0,\tau)$ have their peaks at the same retarded time τ_p, for any z. This implies that the peak of the pulse is traveling with the velocity of light c. Figure 9 illustrates the solution (108) obtained by a digital computer.

If one is not too far from threshold, an explicit solution can be found, instead of the implicit solution (108). This is achieved by expanding the initial Eq. (105)

$$\partial\mathcal{I}(z,\tau)/\partial\tau\simeq(\sigma N_0-2\kappa)\mathcal{I}-\sigma N_0\mathcal{I}^2/\mathcal{I}_s\,, \tag{109}$$

which is readily integrated:

$$\mathcal{I}(z,\tau)=\mathcal{I}(0,\tau)\{1+\mathcal{I}_l^{-1}\mathcal{I}(0,\tau)[\exp\{(\sigma N-2\kappa)z\}-1]\}^{-1} \times\exp\{(\sigma N-2\kappa)z\}\,, \tag{110}$$

where

$$\mathcal{I}_l=[(\sigma N_0-2\kappa)/(\sigma N_0)][\gamma/(2\sigma)] \tag{111}$$

is the limiting photon flux according to the approximate Eq. (109). We see that this value of the limiting photon flux differs from the exact one (107) by a factor of $\sigma N_0/(2\kappa)$ which is close to unity around threshold.

Case 2. Pulse duration short compared to atomic decay times. $(1/\gamma_{ab}\ll\Delta\tau_0\ll1/\gamma_a,\ 1/\gamma_b)$. In this case, the γ_a and γ_b terms are neglected in Eqs. (99), and one obtains

$$\partial\mathcal{I}/\partial z=-2\kappa\mathcal{I}+\sigma\mathcal{I}N\,, \tag{112a}$$

$$\partial N/\partial\tau=-2\sigma\mathcal{I}N\,, \tag{112b}$$

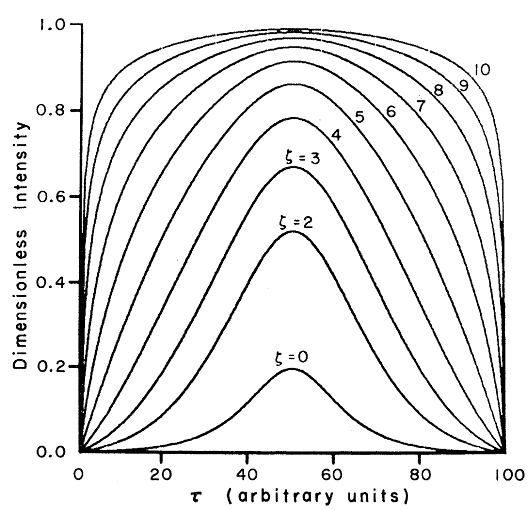

FIG. 9. Evolution of a long pulse as it travels into the medium. The parameter $\sigma N_0/2\kappa$ is fixed at 2.0. The dimensionless intensity $(2\sigma/\gamma)\mathcal{I}$ is plotted versus the retarded time and the successive curves correspond to increasing depths in the medium labelled by values of the dimensionless distance $\zeta=2\kappa z$.

with

$$N=\rho_{aa}-\rho_{bb}. \tag{113}$$

Integrating (112b) and substituting into (112a) we have

$$\partial\mathcal{I}/\partial z=\left[\sigma N_0 \exp\left\{-2\sigma\int_{-\infty}^{\tau}\mathcal{I}(z,\tau')d\tau'\right\}-2\kappa\right]\mathcal{I}. \tag{114}$$

This equation is of the form: rate of change of $\mathcal{I}$ $=$(effective gain$-$loss)$\times\mathcal{I}$, with effective gain$=$gain $\times$saturation factor. We have allowed the signal to be off-resonance by an amount $\omega-\nu$. This detuning reduces the cross section according to (100) which in turn reduces the gain σN_0, but also diminishes the effect of the saturation factor

$$\exp\left(-2\sigma\int_{-\infty}^{\tau}\mathcal{I}d\tau'\right).$$

This result should be expected since off-resonance atoms are harder to saturate.

The evolution of a pulse according to Eq. (114) has been discussed by Basov *et al.*[7] Analytic solutions also have been proposed[5,14,15] for the case $\kappa=0$, but the loss plays an important role in the dynamics of the pulse.

Some insight is gained by first studying the stationary solutions of (114). Such a solution is of the form

$$\mathcal{I}(z,t)=\mathcal{I}(t-z/v)=\mathcal{I}(\bar{\tau}), \tag{115}$$

which represents a pulse moving with velocity v and with unchanging shape. $\mathcal{I}(\bar{\tau})$ obeys

$$(c^{-1}-v^{-1})d\mathcal{I}/d\bar{\tau}=\left\{\sigma N_0\exp\left[-2\sigma\int_{-\infty}^{\bar{\tau}}\mathcal{I}(\tau')d\tau'\right]-2\kappa\right\}\mathcal{I}. \tag{116}$$

Define the quantity

$$R(\bar{\tau})=\int_{-\infty}^{\bar{\tau}}\mathcal{I}(\tau')d\tau', \tag{117}$$

which is the number of photons in the pulse per units area which have already passed for the given value of $\bar{\tau}$.

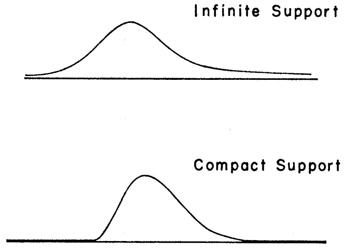

FIG. 10. Illustration of the notion of support of a function.

[14] R. Bellman, G. Birnbaum, and W. G. Wagner, J. Appl. Phys. 34, 780 (1963).
[15] E. O. Schulz-DuBois, Bell System Techn. J. 43, 625 (1964).

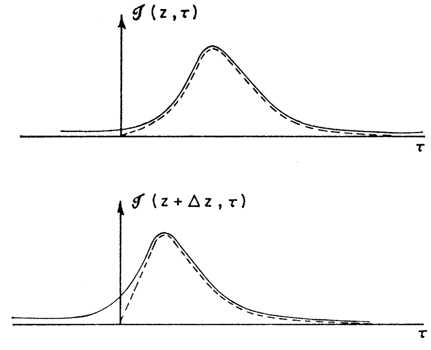

FIG. 11. The upper diagram shows by a solid curve an idealized stationary solution of Eq. (114), for fixed z, and (dotted line) a transient solution approaching the former. The lower figure shows the same situation for a larger value of z. By definition the stationary solution is unchanged in shape but translated to the left since its velocity exceeds c. On the other hand the dotted transient solution is constrained to vanish for $\tau<0$.

Equation (116) may be written in terms of $R(\bar{\tau})$ as

$$(c^{-1}-v^{-1})d^2R/d\bar{\tau}^2=[\sigma N_0\exp(-2\sigma R)-2\kappa]dR/d\bar{\tau}. \tag{118}$$

Integrating this equation with the initial condition

$$(dR/d\bar{\tau})_{\bar{\tau}=-\infty}=\mathcal{I}(-\infty)=0, \tag{119}$$

we get

$$(c^{-1}-v^{-1})dR/d\bar{\tau}=\tfrac{1}{2}N_0[1-\exp(-2\sigma R)]-2\kappa R. \tag{120}$$

We now show that the velocity v of such a stationary pulse must be greater than the velocity of light c if threshold is exceeded. Consider the limit of (120) for $\bar{\tau}\to-\infty$. Since $R(\bar{\tau})\to 0$ as $\bar{\tau}\to-\infty$, we have

$$(c^{-1}-v^{-1})dR/d\bar{\tau}=(\sigma N_0-2\kappa)R. \tag{121}$$

For physically meaningful solutions $dR/d\bar{\tau}=\mathcal{I}$ and R must be positive, so that above threshold we must have $v>c$, A theory predicting signal velocities larger than c would be in contradiction with special relativity. Our theory is based on Maxwell's equations which are relativistically invariant, and on causal quantum mechanics, therefore we would not expect it to make such predictions.

Although Eq. (114) admits stationary solutions propagating faster than light, it can also be seen from (114) that a physical input pulse will never reach such a stationary form. We proceed to prove this statement. A physical pulse should be represented by a function having nonvanishing values only over a finite interval of the τ axis. Such a function will be said to have "compact support" (see Fig. 10). Special relativity sets a limit to the velocity of the first nonvanishing point of the signal. We see from Eq. (120) that the stationary solutions all have infinite support since (120) is analytic and admits only analytic solutions, while a function with compact support cannot be analytic. On the other hand, the transient equation (114) is support conserving

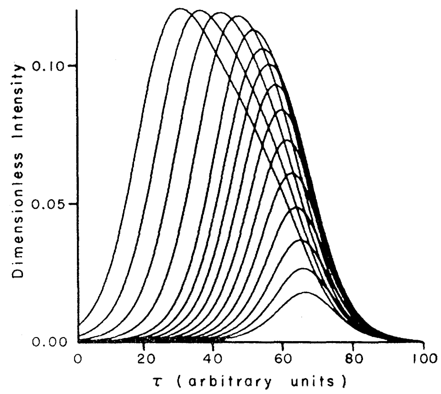

FIG. 12. Evolution of a pulse with infinite tails into a stationary form travelling faster than light, according to Eq. (114), with the following values of the parameters: $\sigma N_0=0.2\ \text{cm}^{-1}$, $2\kappa=0.03\ \text{cm}^{-1}$. The dimensionless intensity $\sigma\mathcal{I}T$ is plotted versus τ/T where T is an arbitrary time unit. The successive curves from right to left correspond to increasing distances into the medium, ranging from $z=0$ to $z=60$ cm.

because $\mathcal{I}=0$ implies $\partial\mathcal{I}/\partial z=0$ and the pulse cannot build up from zero. As a result any physical input pulse has compact support, while the stationary solutions have infinite support and Eq. (114) cannot transform the former into the latter. There remains the possibility of an approximate approach to the stationary state in the sense of Fig. 11(a). This type of an approach can only be temporary. Indeed if one considers Fig. 11(a) at a further distance $z+\Delta z$ [Fig. 11(b)], the stationary solution will have translated to the left by $\Delta z/v$. The actual solution is restricted to the same support and in its tendency to follow the stationary solution will distort its shape and therefore inevitably depart from the stationary form.

Basov *et al.*[7] claim that the numerical integration of Eq. (114) displays a quick approach to the stationary state, but they have integrated (114) with an unphysical input pulse extending to infinity at both ends. They have also measured pulse velocities larger than c, but an experimental apparatus can only trace the bulk of the pulse which may temporarily propagate faster than light without contradicting special relativity.

We have integrated Eq. (114) with a digital computer considering two types of input pulses $\mathcal{I}(0,\tau)$. A pulse with exponential tails like

$$\mathcal{I}(0,\tau)=\mathcal{I}_0\,\text{sech}^2[(\tau-\tau_p)/\Delta\tau_0] \tag{122a}$$

reaches effectively a stationary state as shown in Fig. 12.

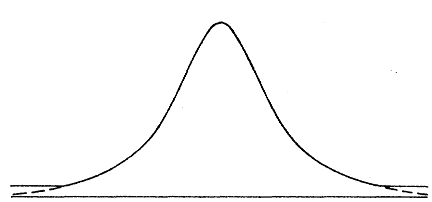

FIG. 13. Truncated hyperbolic secant.

We then alter the above input to give it compact support by simply raising the base line as shown in Fig. 13. The integration with this initial input gives a series of curves properly starting at the origin (see Fig. 14). For a limited time the pulse, except near $\tau=0$, develops towards a stationary form as in the previous case. However this state of affairs cannot go on forever since the pulse must permanently pass through the origin. The numerical integration effectively shows a sudden departure from the quasistationary form with a "piling up" to an increasingly sharper peak near $\tau=0$ (Fig. 15). It is of course understood that the approximations of this section break down when the pulse width is reduced beyond a certain limit. In the next section we will be able to follow the evolution of such a pulse as it becomes too sharp.

In order to demonstrate that the "piling up" is not due to the discontinuities at the junction points $\tau=0$, $\tau=T$, we have also considered input functions of the type

$$\begin{aligned}\mathcal{I}(0,\tau)&=\mathcal{I}_0\exp[-a\tau^{-m}(T-\tau)^{-n}],\quad 0<\tau<T\\&=0\ \text{otherwise}\end{aligned} \tag{122b}$$

which have continuous derivatives to all orders at the junction points. Figure 16 shows the amplification of such a pulse.

B. Moving Atoms—Doppler Broadening (Inhomogeneous Broadening)

Case 1. Pulse duration long compared to atomic-decay times. By the argument given in III B, Eq. (114) generalizes here to

$$\partial\mathcal{I}/\partial z=-2\kappa\mathcal{I}+\sigma_0N_0\mathcal{I}\langle\mathcal{L}(\omega-\nu+Kv)\times[1+(2\sigma_0/\gamma)\mathcal{L}(\omega-\nu+Kv)\mathcal{I}]^{-1}\rangle_v. \tag{123}$$

We have already indicated how to carry out the averaging process involved in this equation. In terms of the parameters ξ, η, and x defined by (75), (76), and

$$x=\eta[1+(2\sigma_0/\gamma)\mathcal{I}]^{1/2}, \tag{124}$$

we obtain

$$\partial\mathcal{I}(z,\tau)/\partial z=[\sigma_0N_0\eta^2x^{-1}Z_i(x+i\xi)-2\kappa]\mathcal{I}, \tag{125}$$

which reduces to

$$\partial\mathcal{I}(z,\tau)/\partial z=[\pi^{1/2}\sigma_0N_0\eta^2x^{-1}e^{x^2}\text{erfc}(x)-2\kappa]\mathcal{I}, \tag{126}$$

when $\xi=(\omega-\nu)/Ku=0$.

Equations (125) and (126) are the counterpart of (80) and (82), but it should be emphasized again that the equations of this section are partial differential equations, while their counterparts in the case of monochromatic waves are ordinary differential equations. The analysis following Eq. (82) applies here with trivial substitutions.

Case 2. Pulse duration short compared to atomic-decay times ($\Delta\tau_0\ll1/\gamma_a$ and $1/\gamma_b$). Here Eq. (114) must be generalized to include the effects of moving atoms. This is accomplished by replacing $\sigma=\sigma_0\mathcal{L}(\omega-\nu)$ by $\sigma=\sigma_0\mathcal{L}(\omega-\nu+Kv)$ since the atomic frequency is Doppler shifted. An average must then be taken over the v dependence of the right-hand side of (114), which gives

$$\partial\mathcal{I}(z,\tau)/\partial z=[\sigma_0N_0\langle\mathcal{L}(\omega-\nu+Kv)\times\exp[-2\sigma_0\mathcal{L}(\omega-\nu+Kv)R]\rangle_v-2\kappa]\mathcal{I}, \quad (127)$$

with

$$R=R(z,\tau)=\int_{-\infty}^{\tau}\mathcal{I}(z,\tau')d\tau'. \quad (128)$$

In general, the average in Eq. (127) cannot be evaluated analytically, but if the velocity distribution in Kv is broad compared to γ_{ab}, as it usually is, then in the limit $\gamma_{ab}/Ku\rightarrow 0$, this integral reduces to

$$\langle\quad\rangle_v=\pi^{-1/2}\int_{-\infty}^{+\infty}\gamma_{ab}^2[\gamma_{ab}^2+(\omega-\nu+Kv)^2]^{-1}\times\exp\{-2\sigma_0R\gamma_{ab}^2[\gamma_{ab}^2+(\omega-\nu+Kv)^2]^{-1}\}d(v/u). \quad (129)$$

We first notice that this average is independent of $\omega-\nu$, which is natural since we assumed a flat velocity distribution. Setting $\omega=\nu$ and $y=Kv/\gamma_{ab}$, the average can be written as

$$\langle\quad\rangle_v=\pi^{-1/2}(\gamma_{ab}/Ku)\int_{-\infty}^{+\infty}(1+y^2)^{-1}\times\exp[-2\sigma_0R(1+y^2)^{-1}]dy. \quad (130)$$

By the change of variable

$$y=\cot(\tfrac{1}{2}\theta), \quad (131)$$

this is transformed into

$$\langle\quad\rangle_v=\pi^{-1/2}\eta e^{-\sigma_0R}\int_0^{\pi}e^{\sigma_0R\cos\theta}d\theta$$
$$=\pi^{1/2}\eta e^{-\sigma_0R}I_0(\sigma_0R), \quad (132)$$

where I_0 is the modified Bessel function of order zero. Substituting this result into (127) we get

$$\partial\mathcal{I}/\partial z=\left\{\pi^{1/2}\sigma_0N_0\eta\exp\left[-\sigma_0\int_{-\infty}^{\tau}\mathcal{I}(z,\tau')d\tau'\right]\times I_0\left[\sigma_0\int_{-\infty}^{\tau}\mathcal{I}(z,\tau')d\tau'\right]-2\kappa\right\}\mathcal{I}. \quad (133)$$

The threshold condition is

$$\pi^{1/2}\sigma_0N_0\eta=2\kappa, \quad (134)$$

indicating that the required value for σ_0N_0 is increased by a factor $\pi^{-1/2}Ku/\gamma_{ab}\gg1$. Otherwise, Eq. (133) leads to the same qualitative behavior as Eq. (114), with a different saturation factor. Compared to a homogenously broadened medium, in the case of Doppler broadening (or inhomogeneous broadening), the gain is smaller for a given density N_0. On the other hand, if the same gain is achieved by increasing N_0, the device amplifies better due to a more favorable saturation factor. Figures 16 and 17 represent solutions of (114) and (133) for the same values of the loss and the gain and with the same input pulse.

Equation (133) also has stationary solutions like (114). A stationary solution of (133) satisfies

$$(c^{-1}-v^{-1})d^2R/d\bar{\tau}^2=[\pi^{1/2}\sigma_0N_0\eta e^{-\sigma_0R}I_0(\sigma_0R)-2\kappa]dR/d\bar{\tau} \quad (135)$$

with

$$\mathcal{I}(z,\tau)=\mathcal{I}(t-z/v)=\mathcal{I}(\bar{\tau}) \quad (136)$$

and

$$R(\bar{\tau})=\int_{-\infty}^{\bar{\tau}}\mathcal{I}(\tau')d\tau'. \quad (137)$$

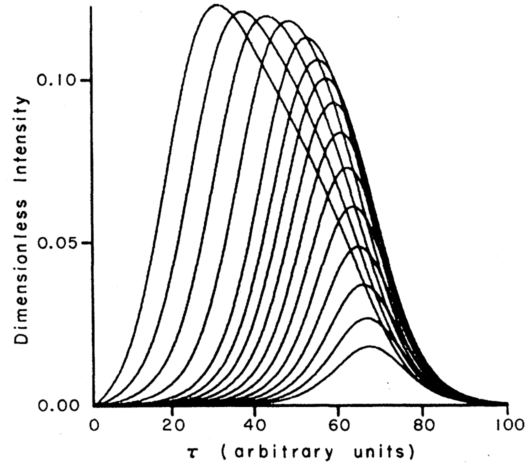

FIG. 14. Integration of Eq. (114) with the same values of the parameters as in Fig. 12, but after truncation of the tails of the input.

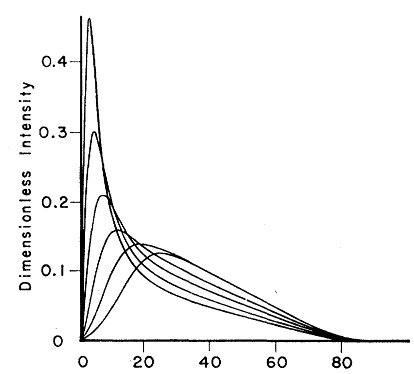

FIG. 15. Extension of Fig. 14 for larger distances into the medium, ranging from $z=60$ to $z=90$ cm by steps of 6 cm.

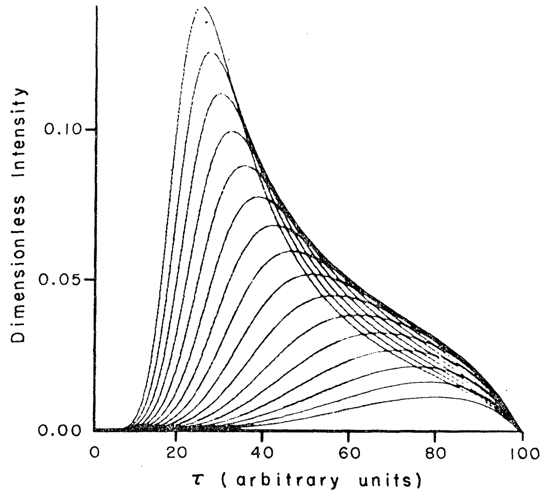

FIG. 16. Integration of Eq. (114) with (122a) as input and with the same values of the parameters as in Fig. 12. The z values range from $z=0$ to $z=45$ cm by steps of 3 cm.

With the initial condition $dR/d\bar{\tau}|_{\bar{\tau}=-\infty}=0$, (135) integrates to

$$(c^{-1}-v^{-1})dR/d\bar{\tau}=\pi^{1/2}\sigma_0 N_0\eta R \times\exp(-\sigma_0 R)[I_0(\sigma_0 R)+I_1(\sigma_0 R)]-2\kappa R, \quad (138a)$$

where I_1 is the modified Bessel function of order one. For $\bar{\tau}\to-\infty$ this equation is approximated by

$$(c^{-1}-v^{-1})dR/d\bar{\tau}\simeq(\pi^{1/2}\sigma_0 N_0\eta-2\kappa)R. \quad (138b)$$

Above threshold $\pi^{1/2}\sigma_0 N_0\eta>2\kappa$, R and $dR/d\bar{\tau}$ are positive for physically meaningful solutions; hence, we must have $v>c$. It is clear from (138a) that such a stationary solution has infinite support and therefore the discussion of IV A Case 2 applies here also.

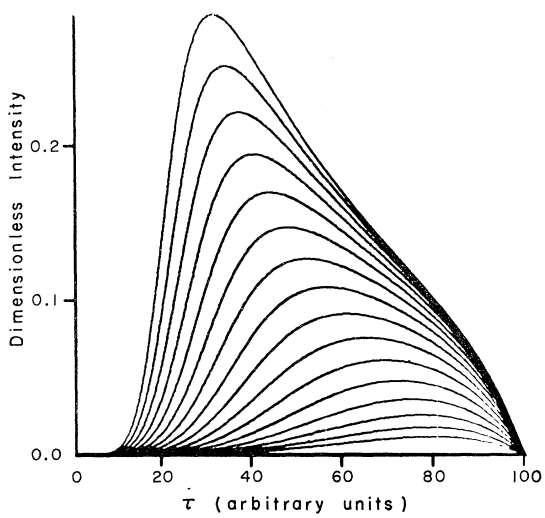

FIG. 17. Effect of Doppler (or inhomogeneous) broadening on pulse propagation. Equation (133) is integrated with the same input pulse, gain and loss parameters and distance range as in Fig. 16. Here we have $Ku\gg\gamma_{ab}$.

V. ULTRASHORT PULSES

In this section we consider pulses much shorter than the atomic phase memory time $1/\gamma_{ab}$, but still much longer than the optical period $2\pi/\nu$. As a consequence the pulse duration is also much shorter than the decay times $1/\gamma_a$, $1/\gamma_b$. The subnsec pulses obtained with gas lasers and the psec pulses produced with solid-state lasers fall under this category.

A. Fixed Atoms

Equations (52) were derived with neglect of variations the field and polarization envelopes and phases in a time $1/\nu$ and a distance $1/K$, and therefore remain valid here. On the other hand, we may now take $\omega=\nu$ without loss of generality since the pulse duration is short enough. Inspection of Eqs. (52) shows that if the input pulse is such that

$$\varphi(0,\tau)\equiv 0, \quad (139)$$

then the phase $\varphi(z,\tau)$, as well as the average in-phase component of the polarization $\langle C\rangle_v$, remains identically zero for any z, provided the velocity distribution is symmetric around $v=0$. Restricting ourselves to "zero phase" input pulses, Eqs. (52) reduce to

$$\partial\mathcal{E}/\partial z=-\kappa\mathcal{E}-\tfrac{1}{2}KS/\epsilon_0, \quad (140a)$$

$$\partial S/\partial\tau=-\gamma_{ab}S-(p^2/\hbar)\mathcal{E}(\rho_{aa}-\rho_{bb}), \quad (140b)$$

$$\partial\rho_{aa}/\partial\tau=\Lambda_a-\gamma_a\rho_{aa}+\tfrac{1}{2}\mathcal{E}S/\hbar, \quad (140c)$$

$$\partial\rho_{bb}/\partial\tau=\Lambda_b-\gamma_b\rho_{bb}-\tfrac{1}{2}\mathcal{E}S/\hbar. \quad (140d)$$

We shall now neglect γ_a, γ_b, and γ_{ab} since the pulse is ultrashort. It was seen that

$$N_0=(\Lambda_a/\gamma_a)-(\Lambda_b/\gamma_b) \quad (141)$$

is the population inversion maintained prior to the arrival of the pulse. If N_0 is to remain finite, in the limit of vanishing γ_a, γ_b we must also take $\Lambda_a=\Lambda_b=0$. Combining the last two equations in (140) we obtain

$$\partial\mathcal{E}/\partial z=-\kappa\mathcal{E}-\tfrac{1}{2}KS/\epsilon_0, \quad (142a)$$

$$\partial S/\partial\tau=-(p^2/\hbar)\mathcal{E}N, \quad (142b)$$

$$\partial N/\partial\tau=\mathcal{E}S/\hbar, \quad (142c)$$

where $N=\rho_{aa}-\rho_{bb}$. The last two equations can easily be integrated, giving

$$S=-pN_0\sin\psi, \quad (143)$$

$$N=N_0\cos\psi, \quad (144)$$

with

$$\psi(z,\tau)=\frac{p}{\hbar}\int_{-\infty}^{\tau}\mathcal{E}(z,\tau')d\tau'. \quad (145)$$

A conservation relation follows as

$$(S/p)^2+N^2=N_0^2. \tag{146}$$

The quantity $\psi(z,\tau)$ is the partial "area" under the pulse envelope at a given space point z. The total area is defined as

$$\theta(z)=\psi(z,+\infty)=\frac{p}{\hbar}\int_{-\infty}^{+\infty}\mathcal{E}(z,\tau')d\tau'. \tag{147}$$

The set of Eqs. (142) is then equivalent to

$$\partial^2\psi/\partial z\partial\tau=-\kappa\partial\psi/\partial\tau+g\sin\psi, \tag{148}$$

where

$$g=\tfrac{1}{2}Kp^2N_0/(\epsilon_0\hbar). \tag{149}$$

The general solution of Eq. (148) is not known. Particular solutions, ignoring the loss term κ, have been constructed by Lamb[6] using the Baeklund transformation. However, the linear loss, although negligible in the problem of an attenuator, plays an important role here.

The evolution of a weak signal according to (148) can be followed analytically, since one has $\psi\ll1$ and (148) can be approximated by

$$\partial^2\psi/\partial z\partial\tau=-\kappa\partial\psi/\partial\tau+g\psi. \tag{150}$$

Differentiating (150) with respect to τ one finds that the field envelope satisfies the same equation

$$\partial^2\mathcal{E}/\partial z\partial\tau=-\kappa\partial\mathcal{E}/\partial\tau+g\mathcal{E}, \tag{151}$$

which is a linear hyperbolic equation with constant coefficients. Given the boundary condition

$$\mathcal{E}(0,\tau)=\mathcal{E}_0(\tau), \tag{152}$$

(151) has a unique solution

$$\mathcal{E}(z,\tau)=e^{-\kappa z}\int_{-\infty}^{\tau}I_0(\{4gz(\tau-\tau')\}^{1/2})\times[d\mathcal{E}_0(\tau')/d\tau']d\tau'. \tag{153}$$

The area function $\psi(z,\tau)$ is given by a similar expression, since it obeys the same equation

$$\psi(z,t)=e^{-\kappa z}\int_{-\infty}^{\tau}I_0(\{4gz(\tau-\tau')\}^{1/2})\mathcal{E}_0(\tau')d\tau'. \tag{154}$$

For large values of τ this integral diverges. The expressions (153) and (154) are therefore valid only for values of τ such that the area as given by (154) is small.

For a strong signal ($\theta\gtrsim1$), the solution (153) can be used to determine the behavior of the pulse in the neighborhood of $\tau=0$, since the initial pulse $\mathcal{E}_0(\tau)$ vanishes for $\tau\leq0$. For small τ we may expand the Bessel function in (154) and get

$$\mathcal{E}(z,\tau)\simeq e^{-\kappa z}\int_0^{\tau}[1+gz(\tau-\tau')][d\mathcal{E}_0(\tau')/d\tau']d\tau'. \tag{155}$$

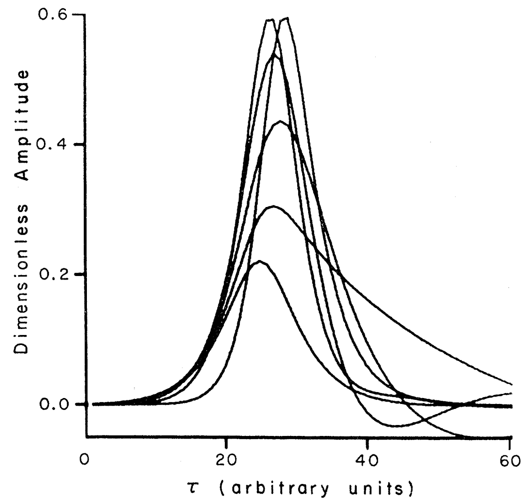

FIG. 18. Propagation of an ultrashort pulse in an unbroadened medium. Equation (148) is integrated with a $\frac{1}{2}\pi$ initial pulse. The dimensionless amplitude $p\mathcal{E}T/\hbar$ is plotted vs τ/T where T is an arbitrary time unit and $gT/\kappa=0.6$. Curves, in order of increasing peak, correspond to distances of 0, 0.4, 1.2, 2.7, 4.0, and 9.5 times the inverse linear loss.

Integrating then by parts we find

$$\mathcal{E}(z,\tau)\underset{\tau\to0}{\simeq}e^{-\kappa z}\left[\mathcal{E}_0(\tau)+gz\int_0^{\tau}\mathcal{E}_0(\tau')d\tau'\right]. \tag{156}$$

If the first term in the Taylor expansion of $\mathcal{E}_0(\tau)$ is of order n, we may write

$$\mathcal{E}_0(\tau)\simeq\tau^n(n!)^{-1}(d^n\mathcal{E}_0/d\tau^n)_0+\tau^{n+1}[(n+1)!]^{-1}\times(d^{n+1}\mathcal{E}_0/d\tau^{n+1})_0. \tag{157}$$

Substituting into (156) we may carry out the integral

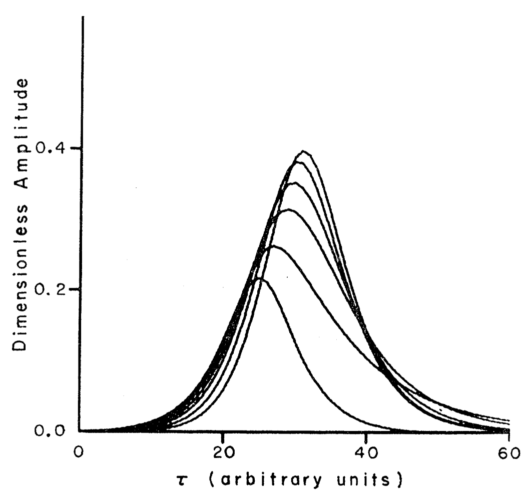

FIG. 19. Effect of nonvanishing γ_{ab} on ultrashort pulse propagation. Equations (171) are integrated with the same input pulse and parameters as in Fig. 13 and with $\gamma_{ab}=0.3$ g/κ. Curves, in order of increasing peak, correspond to distances of 0, 0.8, 1.6, 2.4, 3.2, 4.8 times the inverse linear loss.

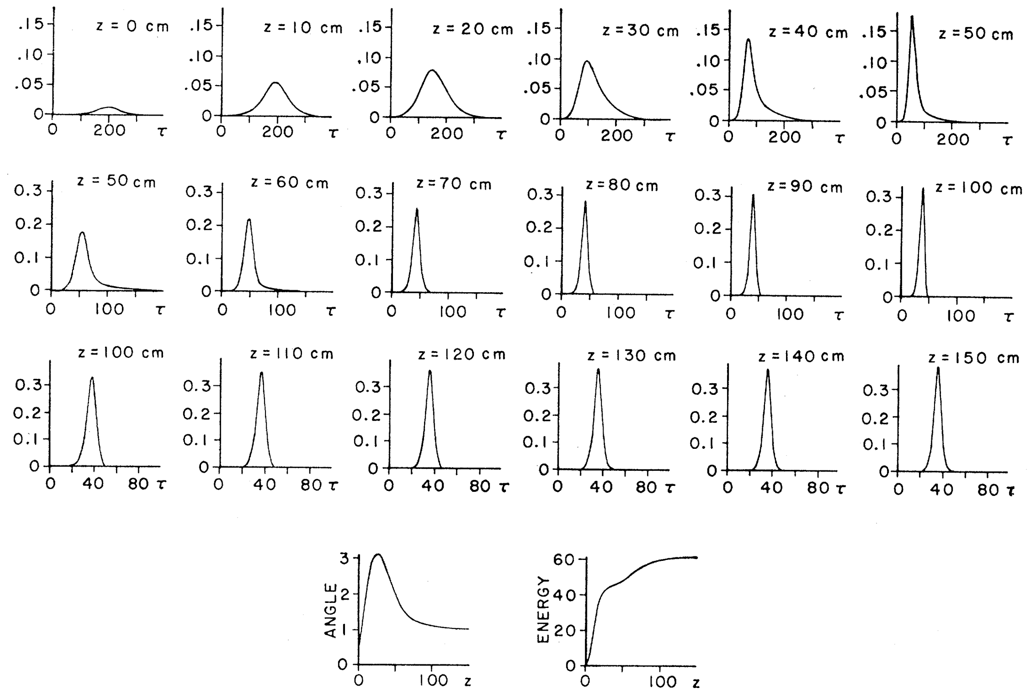

FIG. 20. The series of curves describe the evolution of a $\pi/2$ pulse, initially 100 nsec broad, in a medium with 5 nsec phase memory ($\gamma_{ab}=0.2$ nsec^{-1}). The decay time of the levels a and b is taken to be infinite, and the Doppler broadening is ignored. The quantity $p\mathcal{E}/\hbar$ in nsec^{-1} units is plotted versus τ in nanoseconds. The first curve of each strip duplicates the last curve of the preceeding strip after multiplication of the τ scale by a factor 2. The values of the parameters κ and g are fixed at 0.1 and 0.06. The variation of the angle θ and the energy (in units of the initial energy) as a function of distance is also shown.

and obtain

$$\mathcal{E}(z,\tau) \underset{\tau\to 0}{\simeq} e^{-\kappa z}[1+(gz\tau/n+1)]\mathcal{E}_0(\tau)+O(\tau^{n+2}). \quad (158)$$

We see from this expression that for small τ the effect of the linear loss is dominant since the effect of nonlinear gain is of higher order.

It is possible to find solutions of the exact equation (148) in the form of pulses whose temporal shapes do not change as they travel into the medium. These have the form

$$\psi(z,\tau)=\Psi(\tau-\Delta(z)). \quad (159)$$

The function $\Delta(z)$ represents the amount of time lag associated with z. In terms of the pulse velocity $v(z)$ it can be written as

$$\Delta(z)=\int_0^z [v(z)^{-1}-c^{-1}]dz. \quad (160)$$

Transforming to new variables

$$\tau'=\tau-\Delta(z), \quad (161)$$

$$z'=z, \quad (162)$$

Eq. (148) becomes

$$[\partial^2\psi'(z',\tau')/\partial z'\partial\tau']-[d\Delta(z')/dz'][\partial^2\psi'(z',\tau')/\partial\tau'^2] = -\kappa\partial\psi'/\partial\tau'+g\sin\psi', \quad (163)$$

where

$$\psi'(z',\tau')=\psi(z,\tau). \quad (164)$$

It is easily seen that particular solutions of the form

$$\psi'(z',\tau')=\Psi(\tau') \quad (165)$$

do not exist unless

$$d\Delta(z')/dz'=\text{const}, \quad (166)$$

or

$$v(z)=v. \quad (167)$$

We have thus shown that if a solution with unchanging shape exists, it must travel with a constant velocity. The function $\Psi(\tau)$ must then satisfy

$$(v^{-1}-c^{-1})d^2\Psi/d\tau^2-\kappa d\Psi/d\tau+g\sin\Psi=0. \quad (168)$$

For the physical case $v<c$, (168) is the equation of a pendulum with negative friction which can be thought of as the time reversal image of an ordinary pendulum with positive damping. It may be seen that such a system admits special "limiting solutions" in the form of π pulses. We shall refer to these as the pendulum solutions.

Numerical integration of the transient Eq. (148) shows that an arbitrary initial pulse evolves asymptotically into an unchanging shape which is a hyperbolic secant with total area π, as shown in Fig. 18. It is easily seen from (168) that this corresponds to $v=c$. Equation (168) then becomes

$$\kappa\dot{\Psi}=g\sin\Psi \tag{169}$$

giving

$$(p/\hbar)\mathcal{E}(\tau)=(g/\kappa)\text{sech}[(g/\kappa)(\tau-\tau_0)], \tag{170}$$

where τ_0 is an arbitrary constant of integration. Although theoretically this solution travels with the velocity of light c, a velocity slightly less than c is observed in the numerical integration, as the curves for successive values of z drift slowly towards increasing values of τ (see Fig. 19). This result is accounted for by the fact that we start with an input pulse $\mathcal{E}_0(\tau)$ which is identically zero for $\tau\leq 0$. The transient equation (148) preserves this feature of the pulse for all z, thus preventing the pulse from ever matching exactly one of the solutions represented in (170). However, for increasing τ_0 the mismatch disappears exponentially, thus "pushing" the pulse towards slightly larger values of τ_0. The pendulum solutions with nonzero "mass" ($v\neq c$) proved to be unstable, evolving into the hyperbolic secant form over sufficiently long distances.

For the case of a finite homogeneous broadening γ_{ab}, we shall prove the existence and display the approach to a stationary shape similar to that met above for $\gamma_{ab}=0$. In this case the equations to be considered are

$$\partial\mathcal{E}/\partial z=-\kappa\mathcal{E}-\tfrac{1}{2}KS/\epsilon_0, \tag{171a}$$

$$\partial S/\partial\tau=-\gamma_{ab}S-(p^2/\hbar)\mathcal{E}N, \tag{171b}$$

$$\partial N/\partial\tau=\mathcal{E}S/\hbar. \tag{171c}$$

For a stationary solution traveling with the velocity of light c, we have $\mathcal{E}(z,\tau)=\mathcal{E}(\tau)$, hence $\partial\mathcal{E}/\partial z=0$ and

$$S=-2(\kappa/K)\epsilon_0\mathcal{E}=-pN_0(\kappa/g)(p\mathcal{E}/\hbar) \tag{172}$$

with g given by (149). Substituting (172) into the right-hand side of (171b) and slightly rewriting (171c), we obtain the generalization of (143) and (144)

$$(\partial/\partial\tau)S/pN_0=-(p\mathcal{E}/\hbar)[(N/N_0)-(\gamma_{ab}\kappa/g)], \tag{173a}$$

$$(\partial/\partial\tau)[(N/N_0)-(\gamma_{ab}\kappa/g)]=(p\mathcal{E}/\hbar)(S/pN_0). \tag{173b}$$

Setting as before

$$\psi(z,\tau)=\frac{p}{\hbar}\int_{-\infty}^{\tau}\mathcal{E}(z,\tau')d\tau', \tag{174}$$

we obtain

$$S/pN_0=-[1-(\gamma_{ab}\kappa/g)]\sin\psi, \tag{175}$$

$$(N/N_0)-(\gamma_{ab}\kappa/g)=[1-(\gamma_{ab}\kappa/g)]\cos\psi. \tag{176}$$

From (172) and (175) we have

$$\dot{\psi}=[(g/\kappa)-\gamma_{ab}]\sin\psi, \tag{177}$$

which integrates to

$$(p/\hbar)\mathcal{E}(\tau)=[(g/\kappa)-\gamma_{ab}]\,\text{sech}\{[(g/\kappa)-\gamma_{ab}]\times(\tau-\tau_0)\}. \tag{178}$$

As before, the pulse shape is a hyperbolic secant and its total area is again π. It now has a smaller peak value and is broader than (170) when $\gamma_{ab}>0$. We have integrated (171) with $\gamma_{ab}=0.1\ g/\kappa$ and $\gamma_{ab}=0.3\ g/\kappa$ and have observed that the solution approaches the steady state (178) [see Fig. 19].

The set of equations (171) can also be used to follow the evolution of pulses of the type considered in paragraph IV A 2. There, the pulse width was assumed to be much shorter than $1/\gamma_a$ and $1/\gamma_b$ but much larger than $1/\gamma_{ab}$, enabling us to set $\gamma_a=\gamma_b=0$ and $\gamma_{ab}=\infty$. Integration of the equations under these conditions showed an increasing sharpening of the pulse leading to a breakdown of the second assumption. We integrated Eqs. (171) with $g/\kappa=0.6$ and $\gamma_{ab}=0.2$ ($T_2=5$ nsec) as in the previous case, but with a much broader initial pulse ($\Delta\tau_0=100$ nsec, $\theta_0=\frac{1}{2}\pi$). The first stage of the evolution confirms the behavior predicted in IV A 2, namely peak velocities temporarily exceeding the velocity of light, but as the pulse gets shorter, it settles down to the stationary form (178) traveling with the velocity of light (see Fig. 20). The peak velocity, if defined by reference to the position of the peak of the field in a diagram of $\mathcal{E}$ as a function of τ, for fixed z, is a misleading concept. Indeed, if $\tau_p(z)$ is the retarded time for which a peak occurs at the space point z, the peak velocity is given by

$$v_p=c[1+cd\tau_p/dz]^{-1}, \tag{179}$$

which may become larger than c if $d\tau_p/dz<0$, or even infinite or negative. The fallacy is the following. A pulse of the form $\mathcal{E}(z,t)$ has a spatial shape at any fixed time, and a temporal shape for any fixed z. The two shapes are independent of each other unless they are both unchanging in which case $\mathcal{E}=\mathcal{E}(t-z/v)$. The velocity of the spatial peak of the pulse can be meaningfully defined, but not the velocity of the temporal peak, especially when the pulse is rapidly changing in shape. The meaning of a temporal peak is that a given apparatus is recording a maximum field and it is conceivable that another apparatus, located at a neighboring position, is also recording a maximum at the same instant, thus giving an "infinite velocity".

B. Doppler Broadening

Specializing again for "zero-phase" solutions, Eqs. (52) for $\gamma_a=\gamma_b=\gamma_{ab}=\Lambda_a=\Lambda_b=0$ reduce to

$$\partial\mathcal{E}(z,\tau)/\partial z=-\kappa\mathcal{E}-\tfrac{1}{2}K\langle S/\epsilon_0\rangle_v, \tag{180a}$$

$$\partial S(v,z,\tau)/\partial\tau=-KvC-(p^2/\hbar)\mathcal{E}N, \tag{180b}$$

$$\partial C(v,z,\tau)/\partial\tau=KvS, \tag{180c}$$

$$\partial N(v,z,\tau)/\partial\tau=\mathcal{E}S/\hbar. \tag{180d}$$

A conservation relation in the form

$$(S/p)^2+(C/p)^2+N^2=N_0^2 \tag{181}$$

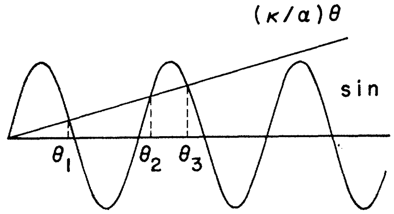

FIG. 21. Graphical determination of the asymptotic values of θ.

is satisfied. As shown in Appendix D, the total area

$$\theta(z)=\frac{p}{\hbar}\int_{-\infty}^{+\infty}\mathcal{E}(z,\tau')d\tau' \tag{182}$$

obeys the "area theorem" of McCall and Hahn[11]

$$d\theta/dz=-\kappa\theta+\alpha\sin\theta, \tag{183}$$

generalized to include the linear loss mechanism. The coefficient α is defined as

$$\alpha=\tfrac{1}{2}\pi(p^2N_0/\epsilon_0\hbar)W(0), \tag{184}$$

where $W(v)$ is the velocity distribution. Note that α is positive for an amplifier and negative for a nonlinear attenuator ($N_0<0$). The area theorem can be thought of as another first integral of the system of equations (180). It expresses the fact that the variation of the area θ depends on θ alone and is not affected by the shape of the field envelope $\mathcal{E}$. Another remarkable property is that this variation is also independent of the detailed velocity distribution $W(v)$. However, it does depend on the value $W(0)$ which usually is related to the width of the distribution.

In the case of fixed atoms the area theorem was not mentioned because the theorem takes a singular form in that limit. Indeed, if we apply the previous result in the limit of an extremely narrow velocity distribution.

$$W(v)\to\delta(v), \tag{185}$$

we have $W(0)=\infty$, hence $\alpha=\infty$, and we find

$$\sin\theta=0,\quad \theta=n\pi. \tag{186}$$

This result is interpreted as follows. Consider an arbitrary input pulse with an arbitrary area $\theta(0)$ at the entry plane $z=0$. At any depth Δz, no matter how small, the area will have reached an integral multiple of π. This unphysical "jump" in θ is a result of the unphysical assumption of no broadening (neither homogeneous nor Doppler), allowing the layer Δz of atoms to ring forever and make a finite contribution to the area.

The solutions $\theta(z)$ of (183) asymptotically approach constant values which are obtained from

$$\sin\theta=(\kappa/\alpha)\theta, \tag{187}$$

giving (see Fig. 21)

$$\theta=\theta_n,\quad (n=1,2,\cdots). \tag{188}$$

If the loss term is small we have

$$\theta_n\simeq n\pi, \tag{189}$$

but this sequence of asymptotic values terminates after approximately $\alpha/\pi\kappa$ values. The solutions of (183) are sketched in Fig. 22. This diagram can be used to follow the evolution of $\theta(z)$ by locating the origin along the z axis to correspond to the initial value of θ. It is seen from Fig. 22 that θ_{2n+1} pulses are stable and θ_{2n} pulses are unstable ($\alpha>0$).

C. Self-Induced Transparency

It can be noted that the area theorem is derived without specifying whether the population is initially inverted or not. For a medium with atoms initially in the ground state (an attenuator), N_0 is negative and the area theorem applies with a negative α

$$d\theta/dz=-\kappa\theta-|\alpha|\sin\theta. \tag{190}$$

Neglecting for simplicity the previously discussed effects of the linear loss terms in this equation, we can sketch the branched solutions as in Fig. 23. For an initial pulse area $\theta_0<\pi$ it is seen that the total area decays to zero. This would be expected on the basis of classical absorption laws. On the other hand if the initial area is

$$\pi<\theta_0<3\pi, \tag{191}$$

the pulse evolves into a 2π pulse, which means that the pulse will not die away over anomalously long distances. This is the "self-induced transparency" effect and has been observed by McCall and Hahn.[11]

Although the area stabilizes at a constant value, it remains to be seen whether the pulse shape can reach a stationary form. In order to investigate this point we shall search for stationary solutions of (180) but we first consider the simple case of fixed atoms by writing Eqs. (171) with $\kappa=0$

$$\partial\mathcal{E}/\partial z=-\tfrac{1}{2}KS/\epsilon_0, \tag{192a}$$

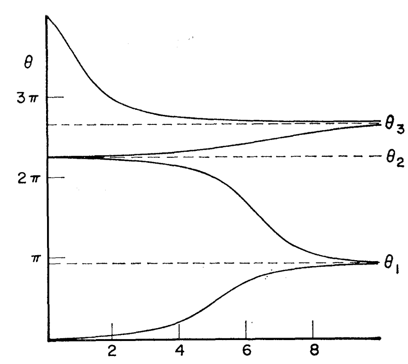

FIG. 22. Branched solutions of the area theorem for an amplifier, Eq. (183), with $\kappa/\alpha=0.1$. The angle θ is plotted vs the dimensionless length αz.

$$\partial S/\partial\tau = -(p^2/\hbar)\mathcal{E}N, \tag{192b}$$

$$\partial N/\partial\tau = \mathcal{E}S/\hbar. \tag{192c}$$

The last two equations are solved by setting

$$S = p|N_0|\sin\psi, \tag{193a}$$

$$N = -|N_0|\cos\psi, \tag{193b}$$

with

$$\psi = p\mathcal{E}/\hbar. \tag{194}$$

A stationary solution propagating with velocity v is of the form

$$\mathcal{E}(z,\tau) = \mathcal{E}(t-z/v) = \mathcal{E}(\tau - z(v^{-1}-c^{-1})). \tag{195}$$

After multiplication by $p\mathcal{E}/\hbar = \dot\psi$, Eq. (192a) gives

$$(\partial/\partial\tau)(p\mathcal{E}/\hbar)^2 = 2g(v^{-1}-c^{-1})\dot\psi\,\sin\psi, \tag{196}$$

with

$$g = \tfrac{1}{2}Kp^2|N_0|/(\epsilon_0\hbar). \tag{197}$$

Integrating (196), subject to the initial conditions $\mathcal{E}(-\infty) = \psi(-\infty) = 0$, and taking the square root we find

$$p\mathcal{E}/\hbar = \dot\psi = (2/\Delta\tau)\sin\tfrac{1}{2}\psi, \tag{198}$$

with

$$\Delta\tau = g^{-1/2}(v^{-1}-c^{-1})^{1/2}. \tag{199}$$

Equation (198) is readily integrated and gives

$$(p/\hbar)\mathcal{E}(z,\tau) = (2/\Delta\tau)\text{sech}\{[t-(z/v)]/\Delta\tau\}, \tag{200}$$

which is a 2π pulse. From (199) the velocity is related to the width through

$$v = c[1+cg(\Delta\tau)^2]^{-1}. \tag{201}$$

A similar result can be proven for the case of Doppler broadening. The proof is more involved and left to Appendix E. As a result it is found that (200) holds with the following width-velocity relation

$$v = c\{1+cg(\Delta\tau)^2\pi^{1/2}(Ku\Delta\tau)^{-1}\exp[(Ku\Delta\tau)^{-2}] \times\text{erfc}[(Ku\Delta\tau)^{-1}]\}^{-1}, \tag{202a}$$

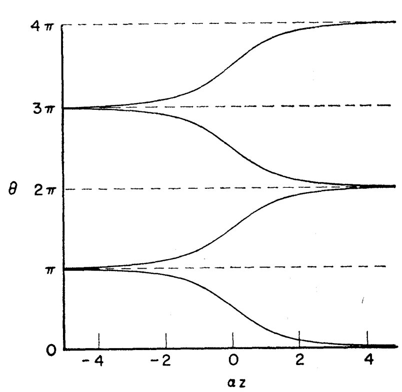

FIG. 23. Branched solutions of the area theorem for an attenuator with $\kappa = 0$.

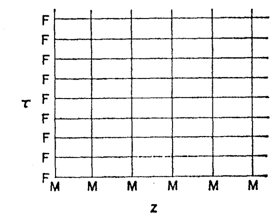

FIG. 24. Rectangular grid used in the numerical integration of Eqs. (226).

which reduces to

$$v = c\{1+\pi^{1/2}cg\Delta\tau/Ku\}^{-1} \tag{202b}$$

for a broad Doppler line ($Ku\Delta\tau \gg 1$).

VI. GENERAL PULSES

In this section we put aside all the assumptions regarding the relative magnitudes of the pulse width and atomic decay times, and derive a set of equations valid in the most general case compatible with the assumptions of the introductory sections. Computer solutions of these equations are then presented and discussed. Although the terminology is appropriate to the case of gas lasers, the equivalence with the problem of a solid state laser should be borne in mind.

A. Transformation of Equations

Without loss of generality we may set $\nu = \omega$ in the basic equations (52) and obtain

$$\partial\mathcal{E}/\partial z = -\kappa\mathcal{E} - \tfrac{1}{2}K\langle S/\epsilon_0\rangle_v, \tag{203a}$$

$$\mathcal{E}\partial\varphi/\partial z = -\tfrac{1}{2}K\langle C/\epsilon_0\rangle_v, \tag{203b}$$

$$\partial S/\partial\tau = -\gamma_{ab}S - (Kv-\dot\varphi)C - (p^2/\hbar) \times\mathcal{E}(\rho_{aa}-\rho_{bb}), \tag{203c}$$

$$\partial C/\partial\tau = -\gamma_{ab}C + (Kv-\dot\varphi)S, \tag{203d}$$

$$\partial\rho_{aa}/\partial\tau = \Lambda_a - \gamma_a\rho_{aa} + \tfrac{1}{2}\mathcal{E}S/\hbar, \tag{203e}$$

$$\partial\rho_{bb}/\partial\tau = \Lambda_b - \gamma_b\rho_{bb} - \tfrac{1}{2}\mathcal{E}S/\hbar. \tag{203f}$$

In the previous discussions the phase equation was neglected by assuming a symmetrical velocity distribution and by restricting the input pulse in such a way that $\varphi(0,\tau) \equiv 0$, thus obtaining the "zero phase" solution $\varphi(z,\tau) \equiv 0$. However it has been shown[12] that if some small $\varphi(0,\tau)$ is injected as input, φ will grow as the wave travels into the medium. It is therefore desirable to introduce this feature into the integration scheme. On the other hand, the phase equation has a singularity for $\mathcal{E} = 0$ which corresponds to the physical fact that the phase is undetermined when the field vanishes. This feature is inconvenient for numerical integration and can be avoided by going over to complex arithmetic in the following way. In Eqs. (203) we make the substitution

$$\mathcal{E}' = \mathcal{E}e^{i\varphi}, \tag{204a}$$

$$\mathcal{P} = -(S+iC)e^{i\varphi}, \tag{204b}$$

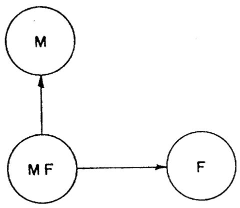

FIG. 25. Schematic representation of the mechanism for propagating the numerical solution.

finding

$$\partial\mathcal{E}'/\partial z=-\kappa\mathcal{E}'+\tfrac{1}{2}K\langle\mathcal{P}/\epsilon_0\rangle_v\,, \tag{205}$$

and

$$\partial\mathcal{P}/\partial\tau=-(\gamma_{ab}-iKv)\mathcal{P}+(p^2/\hbar)\mathcal{E}'N. \tag{206}$$

We also have

$$\mathcal{E}S=\tfrac{1}{2}(\mathcal{E}'\mathcal{P}^*+\mathcal{E}'^*\mathcal{P})\,, \tag{207}$$

so that, omitting the prime on the new complex field $\mathcal{E}'$, Eqs. (203) become

$$\partial\mathcal{E}/\partial z=-\kappa\mathcal{E}+\tfrac{1}{2}K\langle\mathcal{P}/\epsilon_0\rangle_v\,, \tag{208a}$$

$$\partial\mathcal{P}/\partial z=-(\gamma_{ab}-iKv)\mathcal{P}+(p^2/\hbar)\mathcal{E}(\rho_{aa}-\rho_{bb})\,, \tag{208b}$$

$$\partial\rho_{aa}/\partial\tau=\Lambda_a-\gamma_a\rho_{aa}-\tfrac{1}{4}(\mathcal{E}\mathcal{P}^*+\mathcal{E}^*\mathcal{P})/\hbar\,, \tag{208c}$$

$$\partial\rho_{bb}/\partial\tau=\Lambda_b-\gamma_b\rho_{bb}+\tfrac{1}{4}(\mathcal{E}\mathcal{P}^*+\mathcal{E}^*\mathcal{P})/\hbar. \tag{208d}$$

In Eqs. (208) $\mathcal{E}$ and $\mathcal{P}$ are complex quantities but ρ_{aa}, ρ_{bb} are real. This complex field $\mathcal{E}$ has a simple interpretation: its modulus $|\mathcal{E}|$ represents the physical field envelope, and its argument φ the physical phase. Equations (208) are free of singularities and can be easily integrated even with a nonzero initial phase.

B. Numerical Integration Procedure

We now discuss the numerical integration of the system of partial differential Eqs. (208) for the propagation of a pulse through the nonlinear amplifying medium.

If at the entry plane $z=0$ of the medium the incoming pulse is a known function $\mathcal{E}(0,\tau)$, then the last three equations are coupled ordinary differential equations for the variables $\mathcal{P}(v;0,\tau)$, $\rho_{aa}(v;0,\tau)$, $\rho_{bb}(v;0,\tau)$. Given the initial values at $\tau=0$ of these variables, they can be determined for any τ. This calculation is done separately for every velocity v, then the polarization is averaged over velocities giving $\mathcal{P}(0,\tau)$. Actually, only a finite number of representative velocities are used. The choice of these will be discussed later.

For any τ, the first equation gives the evolution in the vicinity of z, of $\mathcal{E}(z,\tau)$ as a function of z since the right-hand side is now known. This permits the determination of the field $\mathcal{E}$ as a function of time τ at some small depth $z+\Delta z$ in the medium. Thus the knowledge of the field is propagated step by step into the laser.

The (z,τ) plane is covered with a rectangular grid, the step sizes Hz along z and $H\tau$ along τ being independently chosen (see Fig. 24). Along $\tau=0$ the medium is unreached by the perturbing pulse and therefore is at rest with known values of the populations and zero polarization. This knowledge is represented by "M" (for medium) at the appropriate points. Similarly the field is assumed known at the entry plane $z=0$. This is indicated by a letter "F" in the diagram. Whenever the field $\mathcal{E}$ and the medium properties $\mathcal{P}$, ρ_{aa}, ρ_{bb} are all known at a lattice point, Eq. (208a) provides the derivative of $\mathcal{E}$ along Oz, and the remaining equations give the derivatives of the medium properties along $O\tau$. Schematically this is represented as shown in Fig. 25. Starting from the origin where we have "MF" we can reach every mesh point as indicated by the diagram of Fig. 25. There are many possible ways of covering the entire lattice, but a natural way of doing this, from a physical point of view, is to procede along successive vertical lines, thus determining the temporal shape of the pulse at successive space points, as would be done by a number of fixed measuring apparatuses located at different points.

The total length of the grid along Oz is of course determined by the length of the medium and the extent along $O\tau$ depends on the initial pulse duration and on how far into the tail of the pulse one wishes to investigate. The time step $H\tau$ is usually chosen to fit 25 points under the initial pulse. The space step Hz is chosen to limit the relative variation of the field at each step.

The actual integration of the equations is performed by the following simple predictor-corrector procedure. If

$$y'=dy/dx=f(y) \tag{209}$$

formally represents the set of equations, with y having several components and x standing for either z or τ, and if y_n is the value of the solution at the nth mesh point along Ox, then

$$p_{n+1}=y_{n-1}+2hy_n' \tag{210}$$

is the predicted value at the $(n+1)$th point, its derivative is

$$p_{n+1}'=f(p_{n+1})\,, \tag{211}$$

and

$$c_{n+1}=y_n+\tfrac{1}{2}h(p_{n+1}'+y_n') \tag{212}$$

is the corrected value. One then takes $y_{n+1}=c_{n+1}$. It is well known that care must be taken in using such predictor-corrector methods since they are not always stable. An integration formula is said to be stable, if the difference sequence Y_n-y_n between the true solution and the approximate solution remains bounded as $n\to\infty$, and can be made as small as one wishes by a suitable choice of the step size h and of the round-off error. Stability is not an intrinsic property of the formula but also depends on the differential system it is being applied to. It is shown in Appendix F that this formula is stable when applied to the system of Eqs. (208).

TABLE I. This table shows the independent parameters that must be fixed when integrating Eqs. (226).

Name	Gain	Loss	Atomic phase memory	Decay consts.	Doppler linewidth	Pumping ratio	Initial pulse width	Initial pulse angle
Symbol	g	κ	γ_{ab}	γ_a,γ_b	Ku	$(\Lambda_b/\gamma_b)/(\Lambda_a/\gamma_a)$	$\Delta\tau_0$	θ_0
Value	0.06	0.005	0.055	0.1, 0.01	variable	0	variable	variable
Units	$\text{cm}^{-1}\times\text{nsec}^{-1}$	cm^{-1}	nsec^{-1}	nsec^{-1}	nsec^{-1}	none	nsec	none

It can be noticed that the predictor-corrector formula calls for two backwards points, which means that we need to know the values of the field $\mathcal{E}$ along two vertical lines (see Fig. 24) and the values of the medium properties along two horizontal lines, before we can start using the formula. The state of the medium is known at any time prior to $\tau=0$, therefore we only need to determine the field along the vertical line adjacent to $z=0$. This is done by using

$$p_{n+1}=y_n+hy'_{n-1} \qquad (213)$$

instead of the predictor formula (210), and by iterating the corrector formula (212) to convergence, in order to make up for the poor accuracy of (213).

C. Averaging over the Velocities

An important aspect of the program is the averaging of the polarization after each space step. The partial polarization $\mathcal{P}(v,z,\tau)$ is first calculated for each velocity v, along the mesh points of the same vertical line of Fig. 24, then an average is taken which approximates as nearly as possible the integral

$$\pi^{-1/2}\int_{-\infty}^{+\infty}\exp\left(-\frac{v^2}{u^2}\right)\mathcal{P}(v,z,\tau)d\frac{v}{u} \qquad (214)$$

by using a finite sum over discrete velocities. For a given number of discrete velocities, this is best achieved by the Hermite-Gauss integration formula of order n

$$\pi^{-1/2}\int_{-\infty}^{+\infty}\exp\left(-\frac{v^2}{u^2}\right)\mathcal{P}(v,z,\tau)d\frac{v}{u} = \sum_{i=1}^{n}\mathcal{P}(v_i,z,\tau)W_i+R_n, \qquad (215)$$

where

$$v_i=ux_i, \quad i=1,\cdots,n \qquad (216)$$

are proportional to the n zeros x_i of the nth Hermite polynomial $H_n(x)$. The weight factors W_i are given by

$$W_i=2^{n-1}n!n^{-2}[H_{n-1}(x_i)]^{-2}, \qquad (217)$$

and the remainder is

$$R_n=[2^{-n}n!/(2n)!]u^{2n}(\partial^{2n}/\partial v^{2n})\mathcal{P}(v,z,\tau). \qquad (218)$$

The $2n$th derivative in this last expression must be evaluated for some typical v which we will take to be u. The zeros of the Hermite polynomials, together with the corresponding weight factors, have been tabulated[16] for n up to 64.

If an upper bound is found for $u^{2n}(\partial^{2n}/\partial v^{2n})\mathcal{P}(v,z,\tau)$ one can see from (218) that by choosing n sufficiently large one may achieve any desired accuracy. We proceed to obtain such an upper bound. By integration of (208b) we obtain

$$\mathcal{P}(v,z,\tau)=\frac{p^2}{\hbar}\int_0^\tau d\tau'\mathcal{E}(z,\tau')N(v,z,\tau') \times\exp[-(\gamma_{ab}-iKv)(\tau-\tau')]; \qquad (219)$$

hence, if we neglect the variation of N with v,

$$|u^{2n}(\partial^{2n}/\partial v^{2n})\mathcal{P}(v,z,\tau)| = \left|(p^2/\hbar)\int_0^\tau d\tau'\mathcal{E}(z,\tau')N(v,z,\tau')[iKu(\tau-\tau')]^{2n} \times\exp[-(\gamma_{ab}-iKv)(\tau-\tau')]\right| \leq (p^2/\hbar)(\mathcal{E}N)_{\max} \times\int_0^\tau d\tau'[Ku(\tau-\tau')]^{2n}$$

$$=(p^2/\hbar Ku)(\mathcal{E}N)_{\max}(Ku\tau)^{2n+1}/(2n+1), \qquad (220)$$

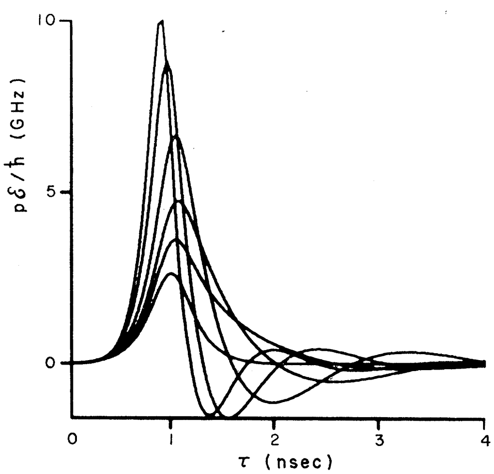

FIG. 26. Standard case. Here, Eqs. (226) are integrated with the following values of the parameters: $\Delta\tau_0=0.5$ nsec, $\theta_0=\frac{1}{2}\pi\rho$, $Ku=1.4$ GHz, all other parameters being fixed as shown in Table I. Curves, in order of increasing peak, correspond to distances of 0, 0.66, 1.32, 2.64, and 3.96 m into the medium.

[16] T. S. Shao, T. C. Chen, and R. M. Frank, Math. Comp. 18, 598 (1964).

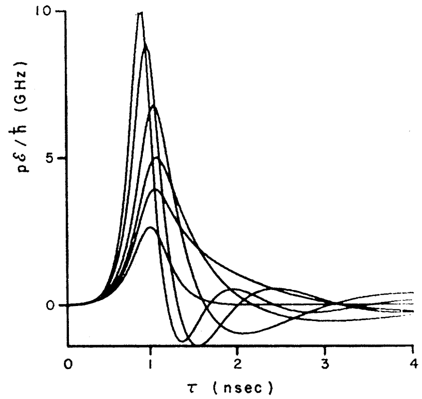

FIG. 27. Fixed atoms. Here, the same situation is represented as in Fig. 26, except for $Ku=0$ instead of $Ku=1.4$ GHz.

where $(\mathcal{E}N)_{\max}$ is the maximum for fixed z of $\mathcal{E}N$ as a function of τ. We find thus

$$R_n \leq (p^2/\hbar Ku)(\mathcal{E}N)_{\max}(Ku\tau)^{2n+1}2^{-n}n!/(2n+1)!. \quad (221)$$

On the other hand we see from (208b) that

$$(p^2/\hbar Ku)(\mathcal{E}N)_{\max} \sim \mathcal{P}(u,z,\tau)_{\max}, \quad (222)$$

so that this quantity may be used as reference in defining a relative error

$$R_n/\mathcal{P}_{\max} \leq 2^{-n}n!(Ku\tau)^{2n+1}/(2n+1)!. \quad (223)$$

The expression (223) is a very satisfactory estimate of the error when $Ku\tau \gg 1$ or $Ku\tau \sim 1$. For $Ku\tau \gg 1$ it tends to overestimate the error. In this case better but more complicated estimates can be found, however (223) will be sufficient for our purposes.

Examination of (223) shows that for $Ku\tau < 1$, one gets excellent accuracy even with a small number of velocities. The relative error (and the number of velocities needed for accurate integration) grows with τ, which means that the effects of Doppler (or inhomogeneous) broadening manifest themselves mainly in the tail of the pulse. In a typical application, the Doppler width may be $Ku=10^9$ Hz and the time of integration $\tau \simeq 5 \times 10^{-9}$ sec, so that the number of velocities needed to achieve $R/\mathcal{P}_{\max} < 0.0001$ is 20. In most practical applications we shall restrict ourselves to "zero phase" input pulses. This implies that the real part of $\mathcal{P}$ will be an even function of v, and since the integrating velocities v_i are symmetrically distributed around $v=0$, the actual number of velocities used is reduced by a factor two.

D. Scaling Laws of Equations

In order to determine the number of independent parameters in Eqs. (208), we make the substitutions

$$p\mathcal{E}/\hbar \to \mathcal{E}, \quad \mathcal{P}/pN_0 \to \mathcal{P}, \quad \rho/N_0 \to \rho \quad (224)$$

with

$$N_0 = (\Lambda_a/\gamma_a) - (\Lambda_b/\gamma_b), \quad (225)$$

and Eqs. (208) become

$$\partial\mathcal{E}/\partial z = -\kappa\mathcal{E} + g\langle\mathcal{P}\rangle_v, \quad (226a)$$

$$\partial\mathcal{P}/\partial\tau = -(\gamma_{ab} - iKv)\mathcal{P} + \mathcal{E}(\rho_{aa} - \rho_{bb}), \quad (226b)$$

$$\partial\rho_{aa}/\partial\tau = (\Lambda_a/N_0) - \gamma_a\rho_{aa} - \tfrac{1}{4}(\mathcal{E}\mathcal{P}^* + \mathcal{E}^*\mathcal{P}), \quad (226c)$$

$$\partial\rho_{bb}/\partial\tau = (\Lambda_b/N_0) - \gamma_b\rho_{bb} + \tfrac{1}{4}(\mathcal{E}\mathcal{P}^* + \mathcal{E}^*\mathcal{P}), \quad (226d)$$

with

$$g = GK\gamma_{ab}, \quad (227)$$

where G is the dimensionless coupling constant given by (65). In (226) $\mathcal{P}$ and ρ are dimensionless, while $\mathcal{E}$ has the dimensions of an inverse time. If the gain coefficient $\mathcal{G}$ of the medium is defined as the inverse length over which

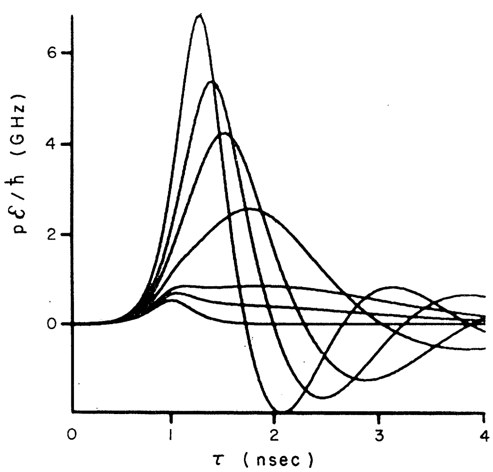

FIG. 28. Weaker pulse. Equations (226) are integrated with the same values of the parameters as in the standard case of Fig. 26, except for $\theta_0 = \pi/10$ instead of $\theta_0 = \frac{1}{2}\pi$. Curves, in order of increasing peak, correspond to distances of 0, 0.22, 0.38, 0.82, 1.35, 1.80, and 2.56 m into the medium.

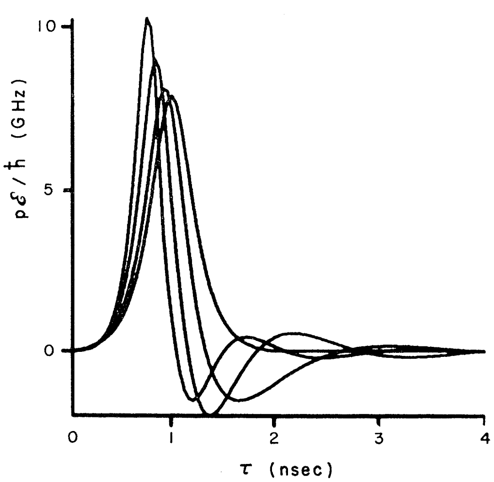

FIG. 29. Stronger pulse. Here the initial pulse angle is $\theta_0 = \frac{1}{2}3\pi$. all other parameters being as in the standard case (see Fig. 26), The four curves in order of increasing peak, represent the pulse as seen at distances of 0, 0.56, 1.70, and 3.38 m into the medium.

a weak monochromatic wave is amplified by a factor e, it follows from Sec. III that

$$\begin{aligned} \mathcal{G} &= \pi^{1/2} g / Ku, \quad \text{for } Ku \gg \gamma_{ab} \\ &= g/\gamma_{ab}, \quad \text{for } \gamma_{ab} \gg Ku. \end{aligned} \tag{228}$$

The independent parameters for Eqs. (226) can be taken to be

$$g, \kappa, Ku, \gamma_{ab}, \gamma_a, \gamma_b, r = (\Lambda_a/\gamma_a)(\Lambda_b/\gamma_b).$$

E. Numerical Results

We proceed to illustrate the use of Eqs. (226) by numerically integrating them for special choices of the parameters. In Appendix G we describe a FORTRAN IV program for solving these equations. The input pulse is usually assumed to be a hyperbolic secant with truncated tails. The independent parameters of the pulse can then be taken as the width $\Delta\tau_0$ and the angle θ, defined by (147). The values of g and γ_{ab} can be fixed without loss of generality, since they determine the space and time scales. In addition, we also fix, for simplicity, the values of κ, γ_a, γ_b, and r as seen in Table I. Zero-phase input will be assumed in all but one of the examples treated below.

A $\frac{1}{2}\pi$ pulse with 0.5-nsec width traveling in a medium with 1.4-GHz Doppler broadening is taken here as a standard case. The evolution of such a pulse (see Fig. 26) shows a sharpening of the front edge with amplification of the peak power. The trailing edge has an oscillatory behavior with several "undershoots." Figure 27 shows the same pulse traveling in a medium with no Doppler broadening. In this case the history of the pulse is essentially the same except for longer oscillations in the tail. In Fig. 28 the initial pulse is weaker

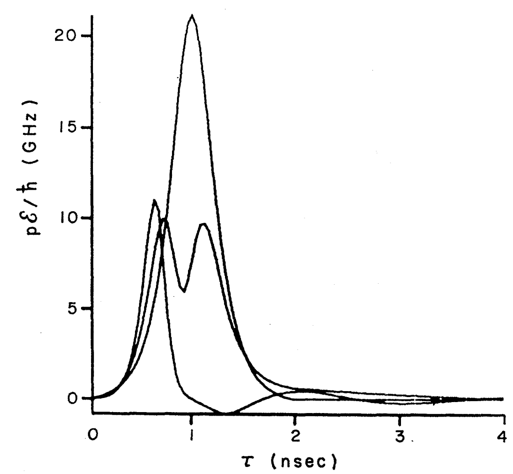

FIG. 30. Pulse breakup. This figure shows how an initially strong pulse ($\theta_0 = 4\pi$) develops more than one peak. The curve with the highest peak represents the initial pulse, the curve with two peaks corresponds to a distance of 1.30 m and the third curve to a distance of 3.60 m into the medium. Apart from θ_0, all other parameters are given the same values as in the standard case of Fig. 26.

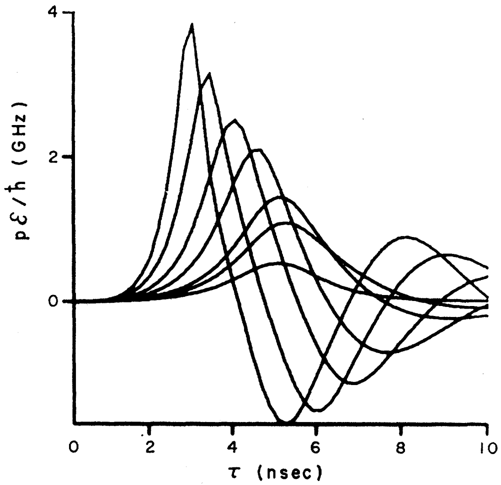

FIG. 31. Broader pulse. Equations (226) are integrated for a pulse initially 2.5 nsec broad, all other parameters having their "standard" values. The increasing peaks belong to pulses located at $z = 0$, 0.14, 0.23, 0.46, 0.68, 1.00, and 1.40 m.

(0.1 π) and in Fig. 29 stronger (1.5 π) compared to the standard case. As would be expected, the weaker the field the more efficient the amplification. Actually, when the initial pulse is too strong (4π) the peak is reduced and the pulse breaks up, as seen in Fig. 30.

We have also considered the effects of varying the pulse width. Figure 31 shows the propagation of a pulse 2.5 nsec broad, other parameters being the same as in the standard case. Larger undershoots are observed. On the other hand, a narrower pulse (0.05 nsec) develops much smaller undershoots (see Fig. 32), undergoes a reduction of the peak, and settles to a stationary form traveling with a velocity less than c. The effect of a larger Doppler linewidth is investigated in this last case.

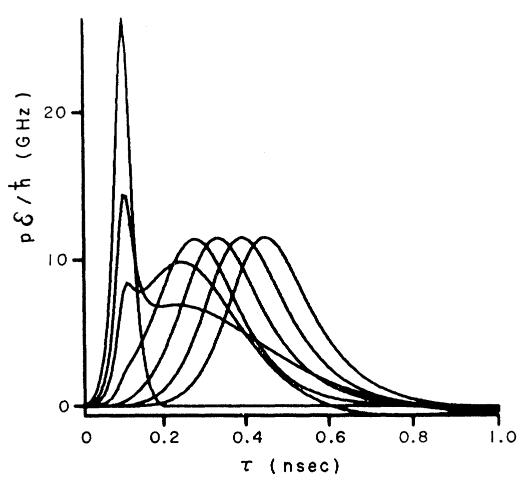

FIG. 32. Sharper pulse. The initial pulse width is taken here to be 0.05 nsec and the other parameters are left unchanged (see Fig. 26). The curve with the highest peak represents the initial pulse. The other peaks from left to right, belong to pulses located at $z = 1.75$, 3.50, 7.00, 12.00, and 21.00 m.

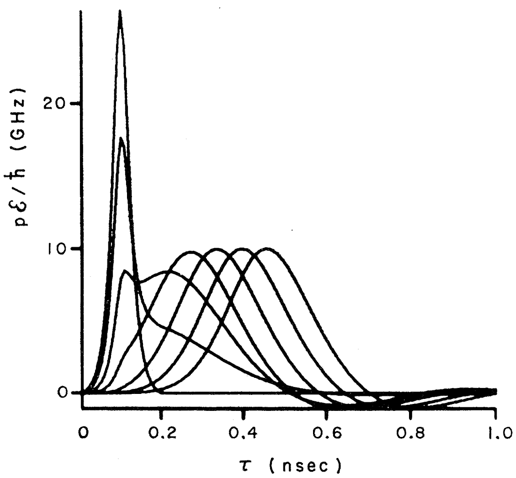

FIG. 33. Broader Doppler line. The calculations of Fig. 32 are repeated here with $Ku=7.0$ GHz instead of $Ku=1.4$ GHz.

Figure 33 describes the same situation as in Fig. 32 except for $Ku=7$ GHz instead of 1.4 GHz. It is seen that the influence of a larger Doppler broadening is not very important. The stationary form is a little broader and the peak is lower.

Finally, we have investigated the effects of a nonzero initial phase $\varphi(0,\tau)$, which for simplicity was taken to be a linear function of time

$$\varphi(0,\tau)=(\omega-\nu)\tau.$$

Such a linear initial phase is equivalent to a detuning of the carrier frequency ν of the pulse from the atomic resonance frequency ω. It was found that a detuning up to Ku has a negligeable effect, but a detuning larger than Ku modifies substantially the evolution of the pulse. This is seen in Fig. 34 which pertains to the standard case with a detuning $(\omega-\nu)=5$ GHz.

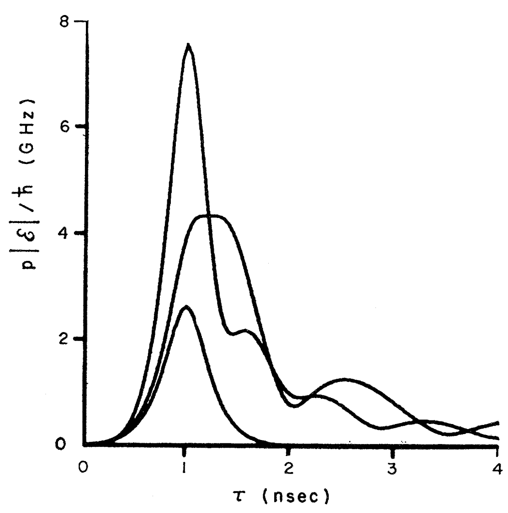

FIG. 34 Effects of detuning. Equations (226) are integrated with the same values of the parameters as in the standard case of Fig. 26, but the carrier frequency of the initial pulse is assumed to be detuned from the atomic resonance frequency by an amount $\omega-\nu=5$ GHz. The three curves, in order of increasing peak, correspond to distances of 0, 1.30, and 3.60 m into the medium.

F. Conclusions

From the calculations we have made it appears that for long enough distances (compared to the inverse gain) the outcoming pulse bears little connection with the input. Over short distances, however, the behavior of the pulse is critically dependent upon its strength as measured by θ and its width. The most general tendency that emerges from the foregoing calculations is for the pulse to develop an oscillating tail. The duration of these oscillations is inversely proportional to the Doppler-width Ku. A strong pulse breaks up into several peaks and undershoots very quickly. On the other hand, a weak pulse is very efficiently amplified and undershoots only after it has gathered sufficient strength. In both cases the total area converges to π. Broad pulses have a tendency to become even broader, while short pulses (compared to $1/\gamma_{ab}$) evolve into quasi-stationary shapes. In the absence of Doppler broadening this stationary shape is usually an hyperbolic secant, but a more complicated form in a Doppler-broadened amplifier. The linear loss κ plays an essential role in the existence of this stationary solution.

We have also checked that as long as the detuning between the carrier frequency of the pulse and the atomic resonance frequency is small compared to Ku, the zero-phase solution remains satisfactory. The amplifier nature of the medium is not affected until this detuning becomes considerably larger than Ku.

APPENDIX A: TRANSFORMATION OF EQS. (30) INTO EQS. (32)

We want to transform Eqs. (30)

$$\partial\rho_{aa}=\lambda_a-\gamma_a\rho_{aa}-i(pE/\hbar)(\rho_{ab}-\rho_{ba}), \quad \text{(A1)}$$

$$\partial\rho_{bb}=\lambda_b-\gamma_b\rho_{bb}+i(pE/\hbar)(\rho_{ab}-\rho_{ba}), \quad \text{(A2)}$$

$$\partial\rho_{ab}=-(\gamma_{ab}+i\omega)\rho_{ab}-i(pE/\hbar)(\rho_{aa}-\rho_{bb}), \quad \text{(A3)}$$

$$\partial\rho_{ba}=-(\gamma_{ab}-i\omega)\rho_{ba}+i(pE/\hbar)(\rho_{aa}-\rho_{bb}), \quad \text{(A4)}$$

where ∂ stands for

$$\partial=(\partial/\partial t)+v(\partial/\partial z), \quad \text{(A5)}$$

to a more convenient form. Define

$$P=p(\rho_{ab}+\rho_{ba}), \quad \text{(A6)}$$

$$Q=p(\rho_{ab}-\rho_{ba}), \quad \text{(A7)}$$

$$N=\rho_{aa}-\rho_{bb}. \quad \text{(A8)}$$

Adding (A3) and (A4) and multiplying by p we get

$$Q=i\omega^{-1}(\partial+\gamma_{ab})P. \quad \text{(A9)}$$

Subtracting (A3) and (A4) multiplying by p and substituting (A9) in the resulting expression we find

$$[(\partial+\gamma_{ab})^2+\omega^2]P=-2\omega(p^2/\hbar)EN. \quad \text{(A10)}$$

On the other hand substituting (A9) into (A3) and (A4) gives

$$\partial\rho_{aa}=\lambda_a-\gamma_a\rho_{aa}+E(\partial+\gamma_{ab})P/\hbar\omega, \quad \text{(A11)}$$

$$\partial\rho_{bb}=\lambda_b-\gamma_b\rho_{bb}-E(\partial+\gamma_{ab})P/\hbar\omega. \quad \text{(A12)}$$

APPENDIX B: SLOWLY VARYING AMPLITUDE AND PHASE APPROXIMATION

If the natural linewidth γ_{ab} is much smaller than the atomic resonance frequency ω, Eqs. (37) may be written as

$$-\partial^2E/\partial z^2+\mu_0\sigma\partial E/\partial t+c^{-2}\partial^2E/\partial t^2=-\mu_0\partial^2P/\partial t^2, \quad \text{(B1)}$$

$$\partial^2P+2\gamma_{ab}\partial P+\omega^2P=-2\omega(p^2/\hbar)E(\rho_{aa}-\rho_{bb}), \quad \text{(B2)}$$

$$\partial\rho_{aa}=\lambda_a-\gamma_a\rho_{aa}+(\hbar\omega)^{-1}E\partial P, \quad \text{(B3)}$$

$$\partial\rho_{bb}=\lambda_b-\gamma_b\rho_{bb}-(\hbar\omega)^{-1}E\partial P, \quad \text{(B4)}$$

where ∂ stands for

$$\partial=(\partial/\partial t)+v(\partial/\partial z). \quad \text{(B5)}$$

Writing the electric field and the polarization as

$$E(z,t)=\mathcal{E}(z,t)\cos\Phi, \quad \text{(B6)}$$

$$P(v,z,t)=C(v,z,t)\cos\Phi+S(v,z,t)\sin\Phi, \quad \text{(B7)}$$

with

$$\Phi=\nu t-Kz+\varphi(z,t), \quad \text{(B8)}$$

we compute the following quantities in the slowly varying amplitude and phase approximation

$$\partial E/\partial t=\dot{\mathcal{E}}\cos\Phi-(\nu+\dot{\varphi})\mathcal{E}\sin\Phi, \quad \text{(B9)}$$

$$\partial^2E/\partial t^2=-2\nu\dot{\mathcal{E}}\sin\Phi-(\nu+\dot{\varphi})^2\mathcal{E}\cos\Phi, \quad \text{(B10)}$$

$$-\partial^2E/\partial z^2=-2K(\partial\mathcal{E}/\partial z)\sin\Phi+[(\partial\varphi/\partial z)-K]^2\mathcal{E}\cos\Phi, \quad \text{(B11)}$$

$$\partial P=\partial C\cos\Phi-C(\nu-Kv+\partial\varphi)\sin\Phi+\partial S\sin\Phi+S(\nu-Kv+\partial\varphi)\cos\Phi, \quad \text{(B12)}$$

$$\partial^2P=-2\nu\partial C\sin\Phi-C(\nu-Kv+\partial\varphi)^2\cos\Phi+2\nu\partial S\cos\Phi-S(\nu-Kv+\partial\varphi)^2\sin\Phi. \quad \text{(B13)}$$

Substituting into the field Eq. (B1) and equating coefficients of $\sin\Phi$ and $\cos\Phi$ we find

$$\partial\mathcal{E}/\partial z+c^{-1}\partial\mathcal{E}/\partial t=-\kappa\mathcal{E}-\tfrac{1}{2}K\int dv\, S/\epsilon_0, \quad \text{(B14)}$$

$$[\partial\varphi/\partial z+c^{-1}\partial\varphi/\partial t]\mathcal{E}=-\tfrac{1}{2}K\int dv\, C/\epsilon_0, \quad \text{(B15)}$$

where

$$\kappa=\tfrac{1}{2}\sigma/(\epsilon_0c). \quad \text{(B16)}$$

We next substitute P in the polarization Eq. (B2), equate coefficients of $\sin\Phi$ and $\cos\Phi$ and obtain

$$\partial C=-\gamma_{ab}C+(\omega-\nu+Kv-\partial\varphi)S, \quad \text{(B17)}$$

$$\partial S=-\gamma_{ab}S-(\omega-\nu+Kv-\partial\varphi)C-(p^2/\hbar)\times\mathcal{E}(\rho_{aa}-\rho_{bb}). \quad \text{(B18)}$$

Neglecting rapidly varying terms, the equations for ρ_{aa} and ρ_{bb} are

$$\partial\rho_{aa}=\lambda_a-\gamma_a\rho_{aa}+\tfrac{1}{2}\mathcal{E}S/\hbar, \quad \text{(B19)}$$

$$\partial\rho_{bb}=\lambda_b-\gamma_b\rho_{bb}-\tfrac{1}{2}\mathcal{E}S/\hbar. \quad \text{(B20)}$$

The source terms λ_α in (B3) and (B4) are velocity-dependent according to

$$\lambda_\alpha=\Lambda_\alpha W(v), \quad \text{(B21)}$$

where $W(v)$ is the velocity distribution function. Taking advantage of the homogeneity of the equations, we shall make the following substitutions

$$\lambda_\alpha\to\Lambda_\alpha, \quad \text{(B22)}$$

and

$$\int S dv\to\int SW(v)dv, \quad \int C dv\to\int CW(v)dv. \quad \text{(B23)}$$

The result can then be summarized as

$$\partial\mathcal{E}/\partial z+c^{-1}\partial\mathcal{E}/\partial t=-\kappa\mathcal{E}-\tfrac{1}{2}K\langle S/\epsilon_0\rangle_v, \quad \text{(B24)}$$

$$[\partial\varphi/\partial z+c^{-1}\partial\varphi/\partial t]\mathcal{E}=-\tfrac{1}{2}K\langle C/\epsilon_0\rangle_v, \quad \text{(B25)}$$

$$\partial S=-\gamma_{ab}S-(\omega-\nu+Kv-\partial\varphi)C-(p^2/\hbar)\times\mathcal{E}(\rho_{aa}-\rho_{bb}), \quad \text{(B26)}$$

$$\partial C=-\gamma_{ab}C+(\omega-\nu+Kv-\partial\varphi)S, \quad \text{(B27)}$$

$$\partial\rho_{aa}=\Lambda_a-\gamma_a\rho_{aa}+\tfrac{1}{2}\mathcal{E}S/\hbar, \quad \text{(B28)}$$

$$\partial\rho_{bb}=\Lambda_b-\gamma_b\rho_{bb}-\tfrac{1}{2}\mathcal{E}S/\hbar, \quad \text{(B29)}$$

where

$$\langle\cdots\rangle_v=\int(\cdots)W(v)dv, \quad \text{(B30)}$$

as stated in Eqs. (44).

APPENDIX C: EVALUATION OF INTEGRAL (78)

Consider

$$I=\int_{-\infty}^{+\infty}[(t+\xi)^2+x^2]^{-1}e^{-t^2}dt. \quad \text{(C1)}$$

Using the integral representation

$$[(t+\xi)^2+x^2]^{-1}= x^{-1}\int_0^\infty e^{-\mu x}\cos\mu(t+\xi)d\mu\,,\quad (x>0) \quad \text{(C2)}$$

we obtain

$$I=x^{-1}\int_{-\infty}^{+\infty}dt\, e^{-t^2}\int_0^\infty d\mu\, e^{-\mu x}\cos\mu(t+\xi)\,, \quad \text{(C3)}$$

and by changing the order of integration

$$I=x^{-1}\int_0^\infty d\mu\, e^{-\mu x}\int_{-\infty}^{+\infty}dt\, e^{-t^2}\cos\mu(t+\xi)\,. \quad \text{(C4)}$$

Expanding the cosine in terms of exponentials we get

$$I=(2x)^{-1}\left\{\int_0^\infty d\mu\, e^{-\mu x+i\mu\xi}\int_{-\infty}^{+\infty}e^{-t^2+i\mu t}dt+\text{c.c.}\right\}. \quad \text{(C5)}$$

Since

$$\int_{-\infty}^{+\infty}e^{-t^2+i\mu t}dt=\pi^{1/2}e^{-\frac{1}{4}\mu^2}, \quad \text{(C6)}$$

we obtain

$$I=\pi^{1/2}(2x)^{-1}\int_0^\infty d\mu\,\exp(-\tfrac{1}{4}\mu^2-\mu x)(e^{i\mu\xi}+e^{-i\mu\xi})\,. \quad \text{(C7)}$$

With the plasma dispersion function defined as

$$Z(\zeta)=i\int_0^\infty \exp(-\tfrac{1}{4}\mu^2-\zeta\mu)d\mu\,, \quad \text{(C8)}$$

we see that

$$I=\pi^{1/2}(2ix)^{-1}\{Z(x+i\xi)+Z(x-i\xi)\} =\pi^{1/2}x^{-1}Z_i(x+i\xi)\,. \quad \text{(C9)}$$

If $\omega=\nu$, we have $\xi=0$ and the integral I reduces to

$$I=\pi^{1/2}x^{-1}\int_0^\infty d\mu\,\exp(-\tfrac{1}{4}\mu^2-\mu x) =2\pi^{1/2}x^{-1}e^{x^2}\int_x^\infty e^{-t^2}dt\,. \quad \text{(C10)}$$

The last integral is defined as the error function[17]

$$\text{erfc}(x)=2\pi^{-1/2}\int_x^\infty e^{-t^2}dt\,, \quad \text{(C11)}$$

[17] *Handbook of Mathematical Functions*, edited by M. Abramowitz and I. A. Stegun (Dover Publications, Inc., New York, 1965).

so that

$$I=\pi x^{-1}e^{x^2}\text{erfc}(x)\,. \quad \text{(C12)}$$

APPENDIX D: DERIVATION OF AREA THEOREM (183)

We here derive the area theorem

$$d\theta/dz=-\kappa\theta+\alpha\sin\theta\,, \quad \text{(D1)}$$

where

$$\theta(z)=\frac{p}{\hbar}\int_{-\infty}^{+\infty}\mathcal{E}(z,\tau')d\tau'\,, \quad \text{(D2)}$$

κ is given by Eq. (45) and α is determined below. Starting with Eqs. (180),

$$\partial\mathcal{E}/\partial z=-\kappa\mathcal{E}-\tfrac{1}{2}K\langle S/\epsilon_0\rangle_v\,, \quad \text{(D3)}$$

$$\partial S/\partial\tau=-KvC-(p^2/\hbar)\mathcal{E}N\,, \quad \text{(D4)}$$

$$\partial C/\partial\tau=KvS\,, \quad \text{(D5)}$$

$$\partial N/\partial\tau=\mathcal{E}S/\hbar\,, \quad \text{(D6)}$$

we integrate (D3) with respect to τ and use (D2) to find

$$d\theta/dz=-\kappa\theta-\tfrac{1}{2}K[p/(\epsilon_0\hbar)]\left\langle\int_{-\infty}^{+\infty}S(v,z,\tau')d\tau'\right\rangle_v. \quad \text{(D7)}$$

From Eq. (D5)

$$S=(Kv)^{-1}\partial C/\partial\tau\,, \quad \text{(D8)}$$

hence,

$$d\theta/dz=-\kappa\theta-\tfrac{1}{2}(p/\epsilon_0\hbar)\lim_{\tau\to\infty}\langle C(v,z,\tau)/v\rangle_v\,. \quad \text{(D9)}$$

The field $\mathcal{E}(z,\tau)$ is supposed to vanish for very large τ, so let τ_0 be such that

$$\mathcal{E}(z,\tau)=0 \quad \text{for} \quad \tau>\tau_0\,, \quad \text{(D10)}$$

then ( ) and ( ) can be integrated to give

$$C(v,z,\tau)=C(v,z,\tau_0)\cos Kv(\tau-\tau_0)+S(v,z,\tau_0) \times\sin Kv(\tau-\tau_0) \quad \text{for } \tau>\tau_0\,. \quad \text{(D11)}$$

We have therefore

$$d\theta/dz=-\kappa\theta-\tfrac{1}{2}[p/(\epsilon_0\hbar)]\lim_{\tau\to\infty}\langle C(v,z,\tau_0)v^{-1} \times\cos Kv(\tau-\tau_0)+S(v,z,\tau_0)v^{-1}\sin Kv(\tau-\tau_0)\rangle_v\,. \quad \text{(D12)}$$

We may interchange the limiting and averaging processes, and using

$$\lim_{\tau\to\infty}v^{-1}\cos Kv(\tau-\tau_0)=\lim_{\tau\to\infty}v^{-1}\sin Kv(\tau-\tau_0)=\pi\delta(v) \quad \text{(D13)}$$

obtain

$$d\theta/dz=-\kappa\theta-\tfrac{1}{2}\pi(p/\epsilon_0\hbar) \times\langle\{C(v,z,\tau_0)+S(v,z,\tau_0)\}\delta(v)\rangle_v\,. \quad \text{(D14)}$$

From Sec. V A we know that

$$C(0,z,\tau_0)=0\,, \tag{D15}$$

$$S(0,z,\tau_0)=-pN_0\sin\psi(z,\tau_0)\,, \tag{D16}$$

hence, if

$$\langle\cdots\rangle_v=\int W(v)(\cdots)dv\,, \tag{D17}$$

we have

$$d\theta/dz=-\kappa\theta+\alpha\sin\psi(z,\tau_0)=-\kappa\theta+\alpha\sin\theta(z)\,, \tag{D18}$$

with

$$\alpha=\tfrac{1}{2}\pi(p^2N_0/\epsilon_0\hbar)W(0)\,. \tag{D19}$$

APPENDIX E: HYPERBOLIC SECANT SOLUTION FOR NONLINEAR ABSORBER

We seek a solution of (180), for an attenuator, in the form of a pulse traveling with unchanging shape

$$\mathcal{E}(z,\tau)=\mathcal{E}(t-z/v)=\mathcal{E}(\bar\tau)\,. \tag{E1}$$

Neglecting the loss term κ, (180a) becomes

$$(c^{-1}-v^{-1})d\mathcal{E}/d\bar\tau=-\tfrac{1}{2}K\langle S/\epsilon_0\rangle_v\,. \tag{E2}$$

The result for the case of homogeneous broadening suggests that we set

$$S(v,z,\tau)=S(0,z,\tau)f(v)=f(v)p|N_0|\sin\psi\,, \tag{E3}$$

so that

$$(p/\hbar)d\mathcal{E}/d\bar\tau=g(v^{-1}-c^{-1})^{-1}\langle f(v)\rangle\sin\psi\,, \tag{E4}$$

where

$$g=\tfrac{1}{2}Kp^2|N_0|/\epsilon_0\hbar\,. \tag{E5}$$

Multiply (E4) by $p\mathcal{E}/\hbar=\dot\psi$, integrate and obtain

$$(p\mathcal{E}/\hbar)^2=4(\Delta\tau)^{-2}\sin^2\tfrac{1}{2}\psi\,, \tag{E6}$$

or

$$p\mathcal{E}/\hbar=\dot\psi=2(\Delta\tau)^{-1}\sin\tfrac{1}{2}\psi \tag{E7}$$

with

$$\Delta\tau=[(v^{-1}-c^{-1})/g\langle f(v)\rangle]^{1/2}\,. \tag{E8}$$

Equation (E7) is readily integrated and gives

$$(p/\hbar)\mathcal{E}(\bar\tau)=2(\Delta\tau)^{-1}\operatorname{sech}(\bar\tau/\Delta\tau)\,. \tag{E9}$$

We now determine $f(v)$ by requiring that the remaining equations in (180) be satisfied. The third equation gives

$$\begin{aligned}\partial C/\partial\tau&=\dot\psi\partial C/\partial\psi=KvS\\&=2(\Delta\tau)^{-1}\sin\tfrac{1}{2}\psi\ \partial C/\partial\psi=p|N_0|Kvf(v)\sin\psi\,,\end{aligned} \tag{E10}$$

hence

$$\partial C/\partial\psi=p|N_0|Kv\Delta\tau f(v)\cos\tfrac{1}{2}\psi\,, \tag{E11}$$

which integrates to

$$C=2p|N_0|Kv\Delta\tau f(v)\sin(\tfrac{1}{2}\psi)\,. \tag{E12}$$

The fourth equation gives

$$\partial N/\partial\tau=\dot\psi\partial N/\partial\psi=\mathcal{E}S/\hbar=\dot\psi S/p\,, \tag{E13}$$

hence

$$\partial N/\partial\psi=|N_0|f(v)\sin\psi\,, \tag{E14}$$

so that

$$N=|N_0|[2f(v)\sin^2(\tfrac{1}{2}\psi)-1]\,, \tag{E15}$$

where the constant of integration has been chosen to satisfy the initial condition $N=-|N_0|$ and $\psi=0$ at $\tau=-\infty$. Substituting S, C, and N into the conservation relation

$$p^{-2}(S^2+C^2)+N^2=N_0^2\,, \tag{E16}$$

we find

$$f(v)[\sin^2\psi+4(Kv\Delta\tau)^2\sin^2(\tfrac{1}{2}\psi)+4\sin^4(\tfrac{1}{2}\psi)]=4\sin^2(\tfrac{1}{2}\psi)\,, \tag{E17}$$

which is readily solved for $f(v)$

$$f(v)=[1+(Kv\Delta\tau)^2]^{-1}\,. \tag{E18}$$

The average of this function is

$$\begin{aligned}\langle f(v)\rangle&=\pi^{-1/2}\int_{-\infty}^{+\infty}e^{-v^2/u^2}[1+(Kv\Delta\tau)^2]^{-1}d(v/u)\\&=\pi^{1/2}(Ku\Delta\tau)^{-1}\exp[(Ku\Delta\tau)^{-2}]\\&\qquad\times\operatorname{erfc}\{(Ku\Delta\tau)^{-1}\}\,,\end{aligned} \tag{E19}$$

so that (E8) gives the following velocity-width relation

$$v=c\{1+cg(\Delta\tau)^2\pi^{1/2}(Ku\Delta\tau)^{-1}e^{(Ku\Delta\tau)^{-2}}\times\operatorname{erfc}[(Ku\Delta\tau)^{-1}]\}^{-1} \tag{E20}$$

as stated in Eq. (202).

APPENDIX F: STABILITY OF INTEGRATION PROCEDURE

We shall only prove the stability of the step-by-step integration of the polarization and populations along the τ axis. The proof is similar and simpler for the integration of the electric field along the z axis. Since the equations are integrated separately for every velocity, it is sufficient to consider a single representative velocity which may be taken to be $v=0$ without loss of generality. Decomposing $\mathcal{E}$ and $\mathcal{P}$ into their real and imaginary parts

$$\mathcal{E}=\mathcal{C}+i\mathcal{S}\,, \tag{F1}$$

$$\mathcal{P}=C+iS\,, \tag{F2}$$

Eqs. (226b), (226c), and (226d) may be written as

$$\partial S/\partial\tau=-\gamma_{ab}S+\mathcal{C}(\rho_{aa}-\rho_{bb})\,, \tag{F3}$$

$$\partial C/\partial\tau=-\gamma_{ab}C-\mathcal{S}(\rho_{aa}-\rho_{bb})\,, \tag{F4}$$

$$\partial\rho_{aa}/\partial\tau=(\Lambda_a/N_0)-\gamma_a\rho_{aa}-\tfrac{1}{2}(\mathcal{C}S-\mathcal{S}C)\,, \tag{F5}$$

$$\partial\rho_{bb}/\partial\tau=(\Lambda_b/N_0)-\gamma_b\rho_{bb}+\tfrac{1}{2}(\mathcal{C}S-\mathcal{S}C)\,. \tag{F6}$$

The above equations can formally be written as

$$\dot{Y}^i = f^i(Y^j), \qquad \text{(F7)}$$

where $Y^i(i=1,2,3,4)$ stands for S, C, ρ_{aa}, ρ_{bb}. If y^i is the approximate solution as opposed to the exact solution Y^i, we define the error

$$\epsilon^i{}_n = Y^i{}_n - y^i{}_n, \qquad \text{(F8)}$$

where n designates the mesh point.

By definition of the approximate solution we have

$$y^i{}_{n+1} = y^i{}_n + \tfrac{1}{2}h(\dot{y}^i{}_{n+1} + \dot{y}^i{}_n) + R^i{}_n, \qquad \text{(F9)}$$

where

$$\dot{y}^i{}_n = f^i(y^i{}_n), \qquad \text{(F10)}$$

and $R^i{}_n$ is the round-off error. On the other hand,

$$Y^i{}_{n+1} = Y^i{}_n + \tfrac{1}{2}h(\dot{Y}^i{}_{n+1} + \dot{Y}^i{}_n) + T^i{}_n, \qquad \text{(F11)}$$

where $T^i{}_n$ is the truncation error. Subtracting (F9) from (F11) we find

$$\epsilon^i{}_{n+1} = \epsilon^i{}_n + \tfrac{1}{2}h(\dot{\epsilon}^i{}_{n+1} + \dot{\epsilon}^i{}_n) + E^i{}_n, \qquad \text{(F12)}$$

where

$$\dot{\epsilon}^i{}_n = \dot{Y}^i{}_n - \dot{y}^i{}_n, \qquad \text{(F13)}$$

and

$$E^i{}_n = T^i{}_n - R^i{}_n. \qquad \text{(F14)}$$

Equation (F13) can be written as

$$\dot{\epsilon}^i{}_n = f^i(Y^j{}_n) - f^i(y^j{}_n) = \epsilon^j{}_n(\partial f^i/\partial y^j)_n, \qquad \text{(F15)}$$

where we used the summation convention. Let

$$f^i{}_j = \partial f^i/\partial y^j, \qquad \text{(F16)}$$

then

$$\epsilon^i{}_{n+1} = \epsilon^i{}_n + \tfrac{1}{2}h(\epsilon^j{}_{n+1} + \epsilon^j{}_n)f^i{}_j + E^i{}_n, \qquad \text{(F17)}$$

or

$$\epsilon^j{}_{n+1}(\delta^i{}_j - \tfrac{1}{2}hf^i{}_j) = \epsilon^j{}_n(\delta^i{}_j + \tfrac{1}{2}hf^i{}_j) + E^i{}_n. \qquad \text{(F18)}$$

Using the matrix notation

$$\delta^i{}_j \pm \tfrac{1}{2}hf^i{}_j = \mathbf{1} \pm \tfrac{1}{2}h\mathbf{f}, \qquad \text{(F19)}$$

Eq. (F18) is solved for $\boldsymbol{\epsilon}_{n+1}$

$$\boldsymbol{\epsilon}_{n+1} = (\mathbf{1} - \tfrac{1}{2}h\mathbf{f})^{-1}(\mathbf{1} + \tfrac{1}{2}h\mathbf{f})\boldsymbol{\epsilon}_n + \mathbf{E}'_n \qquad \text{(F20)}$$

with

$$\mathbf{E}'_n = (\mathbf{1} - \tfrac{1}{2}h\mathbf{f})^{-1}\mathbf{E}_n. \qquad \text{(F21)}$$

If $\mathbf{f}$ is treated as constant in n (this idealization is not necessary but greatly simplifies the proof), and if λ^j are the eigenvalues of $\mathbf{f}$, one can find four linear combinations η^j of the ϵ^i's, such that

$$\eta^j{}_{n+1} = (1 - \tfrac{1}{2}h\lambda^j)^{-1}(1 + \tfrac{1}{2}h\lambda^j)\eta^j{}_n + E^{j\prime\prime}{}_n, \qquad \text{(F22)}$$

where $E^{j\prime\prime}{}_n$ are the same linear combination of the $E^{i\prime}{}_n$ (we shall omit the $''$ and consider $E^j{}_n$ to be the same at every step n). The solution of the difference Eq. (F22) is

$$\eta^j{}_n = C(\rho^j)^n + E^j[1 - (\rho^j)^n][1 - \rho^j]^{-1}, \qquad \text{(F23)}$$

where C is a constant and ρ^j is given by

$$\rho^j = (1 - \tfrac{1}{2}h\lambda^j)^{-1}(1 + \tfrac{1}{2}h\lambda^j). \qquad \text{(F24)}$$

If for all j, $|\rho^j| < 1$, i.e., if $\text{Re}\lambda^j < 0$

$$\lim_{n\to\infty} \eta^j{}_n = E^j(1 - \rho^j)^{-1} < +\infty, \qquad \text{(F25)}$$

therefore $\lim_{n\to\infty} \epsilon^j{}_n$ is also finite for all j since the ϵ's are linear combination of the η's. On the other hand, if $|\rho^j| > 1$ for some j, then at least one $\epsilon^j{}_n$ diverges as $n \to \infty$. Hence, the requirement for stability is

$$|\rho^j| < 1 \quad \text{or} \quad \text{Re}\lambda^j < 0 \quad \text{for all } j. \qquad \text{(F26)}$$

The limiting errors $E^j(1-\rho^j)^{-1}$ can be made as small as one wishes by choosing h small enough, since E^j is of order h^3.

Now we check that $\text{Re}\lambda^j < 0$. For the system of Eqs. (F3)–(F6), the matrix $f^i{}_j$ is by definition [see Eq. (F16)]

$$f^i{}_j = \begin{bmatrix} -\gamma_{ab} & 0 & \mathcal{C} & -\mathcal{C} \\ 0 & -\gamma_{ab} & -\mathcal{S} & \mathcal{S} \\ -\tfrac{1}{2}\mathcal{C} & \tfrac{1}{2}\mathcal{S} & -\gamma_a & 0 \\ \tfrac{1}{2}\mathcal{C} & -\tfrac{1}{2}\mathcal{S} & 0 & -\gamma_b \end{bmatrix} \qquad \text{(F27)}$$

and the characteristic equation is

$$(\gamma_{ab} + \lambda)^2[\mathcal{E}^2 + (\gamma_a + \lambda)(\gamma_b + \lambda)] = 0, \qquad \text{(F28)}$$

where we used $\gamma_{ab} = \tfrac{1}{2}(\gamma_a + \gamma_b)$ for simplicity, and

$$\mathcal{E}^2 = \mathcal{C}^2 + \mathcal{S}^2. \qquad \text{(F29)}$$

The four roots

$$\lambda_1 = \lambda_2 = -\gamma_{ab}, \qquad \text{(F30)}$$

$$\lambda_{3,4} = -\gamma_{ab} \pm [\tfrac{1}{4}(\gamma_a - \gamma_b)^2 - \mathcal{E}^2]^{1/2} \qquad \text{(F31)}$$

are such that $\text{Re}\lambda^j < 0$, and the stability is proven. The fact that $f^i{}_j$ is not constant in n (since the field components $\mathcal{C}$ and $\mathcal{S}$ depend on n) does not change the conclusion. In a more rigorous treatment the power law solution $\eta^j{}_{n+1} \sim (\rho^j)^n$ would be replaced by a product of the form

$$\eta^j{}_n \sim \prod_1^n (\rho^j{}_l) \qquad \text{(F32)}$$

which also converges to zero as $n \to \infty$, since every factor is less than unity.

APPENDIX G: FORTRAN IV PROGRAM

In this appendix we describe the digital computer program we use to integrate Eqs. (225). The essential steps of the program are shown in flow chart form.

The following notation is used in flow charts

$$\tau_n = nHT, \quad n = -1, 0, 1, 2, \cdots, M \qquad \text{(G1)}$$

$$z_j = jHS, \quad j = 0, 1, 2 \qquad \text{(G2)}$$

$$v_k = x_k u, \quad k = 1, 2, 3, \cdots, IS \qquad \text{(G3)}$$

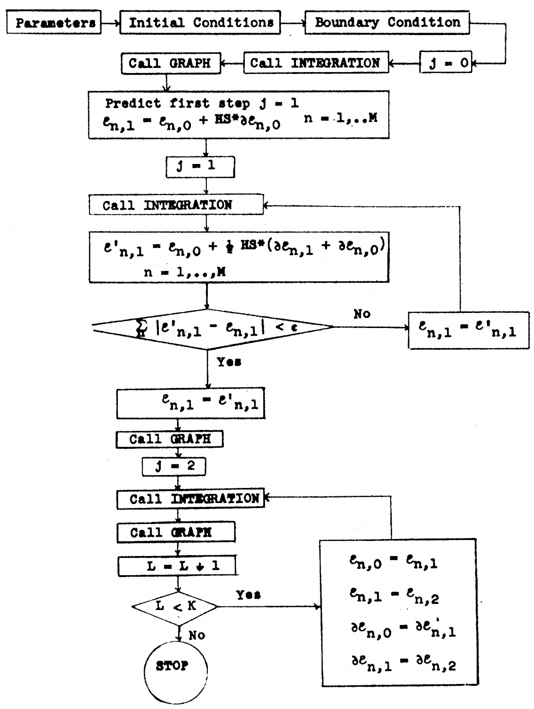

FIG. 35. Flow chart for the MAIN routine. The notation used is explained in Appendix G.

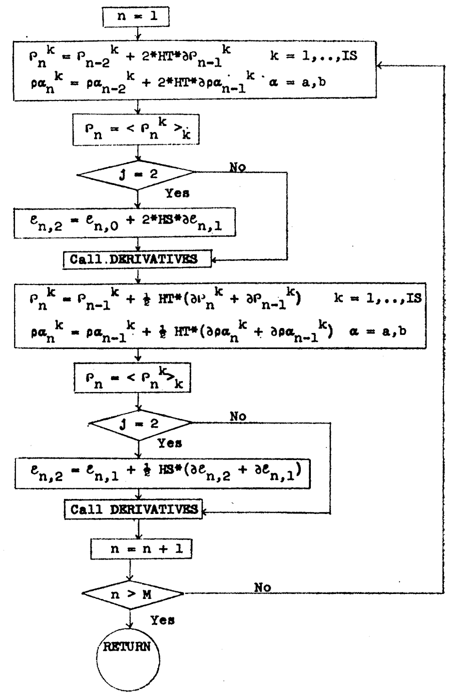

FIG. 36. Flow chart for subroutine INTEGRATION. The notation used is explained in Appendix G.

where HT is the time step size, HS the space step size, M the desired number of time steps in the integration, IS the number of velocities and x_k the zeros of the ISth-order Hermite polynomial,

$$\mathcal{E}_{nj}=\mathcal{E}(\tau_n,z_j)\,, \tag{G4}$$

$$\partial\mathcal{E}_{nj}=\partial\mathcal{E}(\tau_n,z_j)/\partial z\,, \tag{G5}$$

$$\mathcal{P}_{nj}{}^k=\mathcal{P}(v_k,\tau_n,z_j)\,, \tag{G6}$$

$$\partial\mathcal{P}_{nj}{}^k=\partial\mathcal{P}(v_k,\tau_n,z_j)/\partial\tau\,, \tag{G7}$$

$$\rho\alpha_{nj}{}^k=\rho_{\alpha\alpha}(v_k,\tau_n,z_j)\,, \tag{G8}$$

$$\partial\rho\alpha_{nj}{}^k=\partial\rho_{\alpha\alpha}(v_k,\tau_n,z_j)/\partial\tau\,, \tag{G9}$$

$$\mathcal{P}_{nj}=\mathcal{P}(\tau_n,z_j)=\langle\mathcal{P}_{nj}{}^k\rangle_k\,. \tag{G10}$$

The input can be classified as follows:

Parameters contain all independent parameters described in Sec. VI-4, the integrating velocities and their weights (see VI-3).

Initial conditions are common to all applications and express the fact that the pulse hits the entry plane ($z=0$) at time $t=\tau=0$ and until then the medium is at rest with zero polarization and given values of the populations. These conditions are built into the program.

Boundary condition the array $\mathcal{E}_{n,0}(n=1,2,\cdots,M)$ represents the incoming pulse and must be read in.

In addition to the MAIN routine, the program includes three subroutines. Subroutine INTEGRATION contains the predictor-corrector formula and is the core of the program. Subroutine DERIVATIVES contains the equations to be integrated, and subroutine GRAPH is devised to give output in the desired format. Flow charts of MAIN and INTEGRATION are seen in Fig. 35 and Fig. 36.